Dynamics of Glass Forming Materials

by

Astrid Karina Torres Arellano, B.S.

A Thesis

In

Chemical Engineering

Submitted to the Graduate Faculty
of Texas Tech University in
Partial Fulfillment of
the Requirements for
the Degree of

Master of Science

in

Chemical Engineering

Approved

Gregory B. McKenna
Chair of Committee

Rajesh Khare

Sindee Simon

Mark Sheridan
Dean of the Graduate School

May, 2015

ACKNOWLEDGMENTS

I would like to acknowledge the people who have been involved in the culmination of this work. First, I would like to express my greatest gratitude to a great mentor and advisor Dr. Gregory B. McKenna. I would like to say that I felt truly blessed in having Dr. McKenna as my advisor. I want to thank him for all his support, advice, guidance, and constant encouragement through my years of study at Texas Tech University. Under his guidance I was able to grow academically and personally. There are not enough words to express how grateful I have felt for being part of his research group.

I would also like to thank the members of my thesis defense committee, Dr. Sindee Simon and Dr. Rajesh Khare for cordially accepting to be members of my committee. Special thanks to Dr. Sindee Simon for allowing the use of the differential scanning calorimetries, and to Dr. Ronald Hedden for allowing the use of the GPC.

I would like to also express my most sincere gratitude to my dear friend Rutvik Godbole for his friendship, encouragement, and support while at Tech. I really appreciated his companionship and words that helped me stay focused on my goals and work. I would like to also express my gratitude to Heedong Yoon for he was a great lab colleague.

I would like to thank the John R. Bradford Endowment at Texas Tech University and the National Science Foundation under grant DMR-1207070 for their partial support of this work.

Finally, I would like to thank God for He was the one always in my heart. He gave me a wonderful mother that was always there as a friend to listen, to guide, to encourage, to motivate and to help me stay focused in the love of God; to them I dedicate my current thesis. Also, I thank Him because He gave me wonderful friends Paul, Rosbel, Gabriela and Reynaldo (my brother) for they were always there to listen in the times of trouble, to make me laugh, to help me, and to keep me focused on my objectives. I would also like to thank my dad Rolando and my siblings Rolando and Rigo for they always were there to show me their support and love.

TABLE OF CONTENTS

ABSTRACT

The liquid dewetting method was used to study the T_g dependence of ultrathin polymer films on thickness and on molecular architecture. Studies of linear polystyrene (PS), 3-arm star PS, short branched and long branched 8-arm star PS on a liquid substrate (glycerol) were performed by using two built dewetting apparatus. Results show that the T_g vs. film thickness for all of the PS films on glycerol are more similar to that of supported on rigid substrate films than for freely standing films. Additionally, a temperature step (T-step) dewetting method which is an extension of the original liquid dewetting technique idea was investigated. In the temperature step method one single polymer sample can provide the same T_g dependence on thickness information that multiple samples of different thicknesses would give. The idea behind the T-step method test is to control the experimental temperature and use a single polymeric thin film sample within a single experimental run. It was found that linear and 3-arm star PS films have a similar T_g vs. film-thickness dewetting response, while the long and the short branched 8 arm star PS films have a more complex behavior.

The dynamic fragility of glass-forming materials can be obtained by means of calorimetric methods from the T_g dependence on the cooling rate and by rheological methods. Calorimetry is used to investigate reports of extreme fragility values for polysulfone (PSF), bisphenol-A-polycarbonate (PC), and polyvinyl chloride (PVC). The polymers were used as-received and after a wash-precipitation treatment. Results for the fragilities for several materials using both a broad range of cooling rates and a small range of high cooling rates were compared. Results show that the dynamic fragilities of as-received and wash-precipitated polymer samples were consistent with

each other. The results were not in agreement with C. Evans, H. Deng, W. Jager, J. Torkelson, *Macromolecules* **2013**, *46 (15)*, 6091-6103 of extremely high fragility for the mentioned polymers. The wash-precipitation treatment does not play an important role in the determination of the dynamic fragility of the polymers. However, the range of cooling rates does have an effect on the magnitude of *m.* Results show that the dynamic fragility obtained from the broader range of cooling rates tend to give a somewhat lower value of *m*.

Calorimetric and rheological methods were used on D,L-lactic acid to investigate the speculation that this lactic acid should have a very extreme fragility. Results show that the dynamic fragility of D,L-lactic acid and D-lactic acid are not in the range for an extreme fragile material.

LIST OF FIGURES

CHAPTER I

INTRODUCTION AND BACKGROUND

In 1989, McKenna gave a very interesting opening for his chapter in Glass Formation and Glassy Behaviors.[1] He talked about how in about 20 years (from 1968 to 1987) the amount of citations referring to polymer glasses passed over 10,000. His chapter was based on trying to explain the glass transition temperature (T_g) and the kinetics of the glass forming systems.[1] Around 25 years have passed since McKenna's publication and he has continued with his interest in glass forming materials and glass transition behaviors. It was also McKenna along with Jackson[2] who first published studies of how confinement in nanopores for an organic glass forming liquid can result in a depressed T_g. To further understand studies on confined systems, and to better understand the findings on increase, decrease or unchanged T_g. We first start the current work by introducing some main definitions concerning the glass transition temperature, the glass forming materials important aspects as dynamic fragility, and how different confinement techniques have affected the T_g behavior that will later lead us to understand better the significance of the current work on the liquid dewetting technique for determination of T_g of confined polymer systems (thin films) and dynamic fragility of glass-forming materials by calorimetric and rheological methods.

1.1 Glass Transition Temperature (T_g)

The glass transition temperature T_g depends on cooling rate and it is considered to be the temperature at which the molecular mobility gets restrained

(vitrified).[1] For an amorphous polymer above the T_g the material is found to be an amorphous liquid. However, upon cooling the material goes from amorphous liquid to an amorphous glass. This transition occurs when the amorphous liquid polymer, which is in an equilibrium liquid state at high temperature, is cooled down at a given cooling rate to a non-equilibrium state.

The T_g is commonly determined from thermal methods (calorimetric) or dynamic methods. In calorimetry measurements, the heat flow or the heat capacity is required as a function of temperature. The T_g can be obtained from the step change of the heat capacity (Figure 1.1). The T_g is then the point at which the total step change acquires half the value.[3] The T_g can also be determined from the specific volume (V)/enthalpy (H) versus temperature plot (Figure 1.2) for a given polymer. In this case, the T_g is the point of intersection of the extrapolated equilibrium liquid and glassy lines.[3,4] The higher the cooling rate (q) the higher the obtained T_g. This higher T_g for higher q is due to the fact that there is not sufficient time for structural relaxation. Then the system deviates from equilibrium at a higher temperature. Similarly, if the material is cooled at a lower rate, the material has more time for structural relaxation then deviates from equilibrium at a lower specific volume (or enthalpy), resulting in a lower T_g. The T_g determined by dynamic methods (e.g. rheology, dielectric measurements) involves the viscosity (η) or the relaxation time (τ) dependence on temperature.[5] For these particular measurements the Vogel-Fulcher-Tamman (VFT)[6-8] and the William-Landel-Ferry (WLF) equations are required.[9]

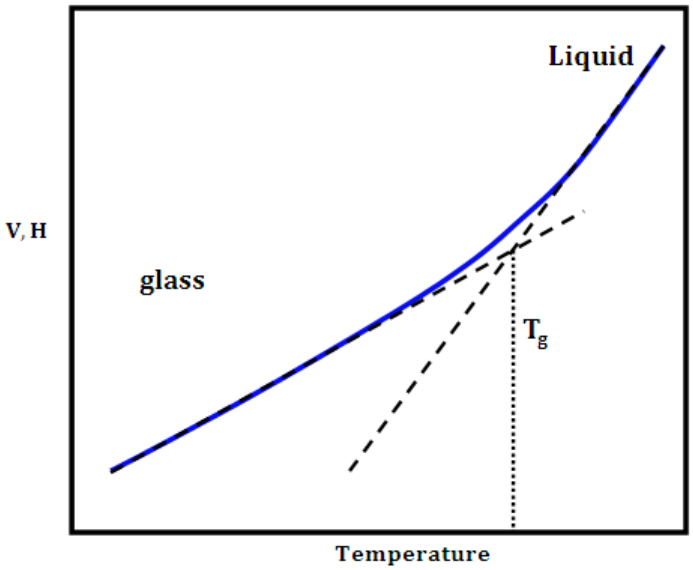

Figure 1.1 Schematic of the specific volume (or enthalpy) vs. the temperature. T_g is found from the intersection point of the liquid and the glass lines.[3]

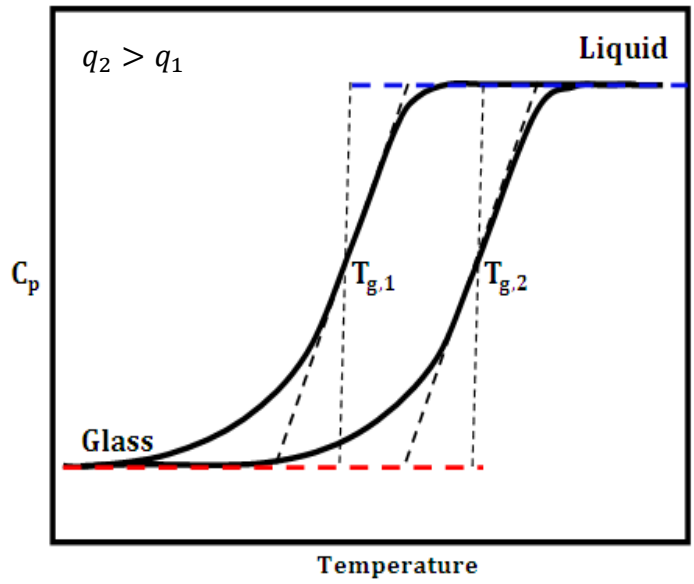

Figure 1.2 Schematic of the heat capacity with temperature for determination of the glass transition temperature. The cooling rate q_2 is associated with $T_{g,2}$ and q_2 is associated with $T_{g,2}$ and q_1 is associated with $T_{g,1}$.

1.2 Fictive Temperature (T_f) and Limiting Fictive Temperature (T_f')

The fictive temperature (T_f) was first introduced by Tool in the 1940s.[10] T_f is used to describe the glassy state.[10] Contrary to the glass transition temperature, the fictive temperature can appropriately be obtained on heating.[3,10] Figure 1.3a shows a typical specific heat (or enthalpy) vs. temperature plot upon heating at a constant rate after the sample was cooled at a rate q. From Figure 1.3a after the material was cooled at cooling rate of q_2, upon heating the material first follows the glass line until it overshoots the equilibrium line and goes back to equilibrium at a higher temperature. The fictive temperature is then found to be the intersection point of the extrapolated liquid and glass lines (in this particular scenario, $T_{f,2}$).[3,10] In Figure 1.3b a schematic of the heat capacity vs. the temperature of a material is shown. The heating scan (the heat capacity curve) overshoots slightly shift to higher temperatures and grow in magnitude with decreasing cooling rates (at lower cooling rates) for a constant heating rate.

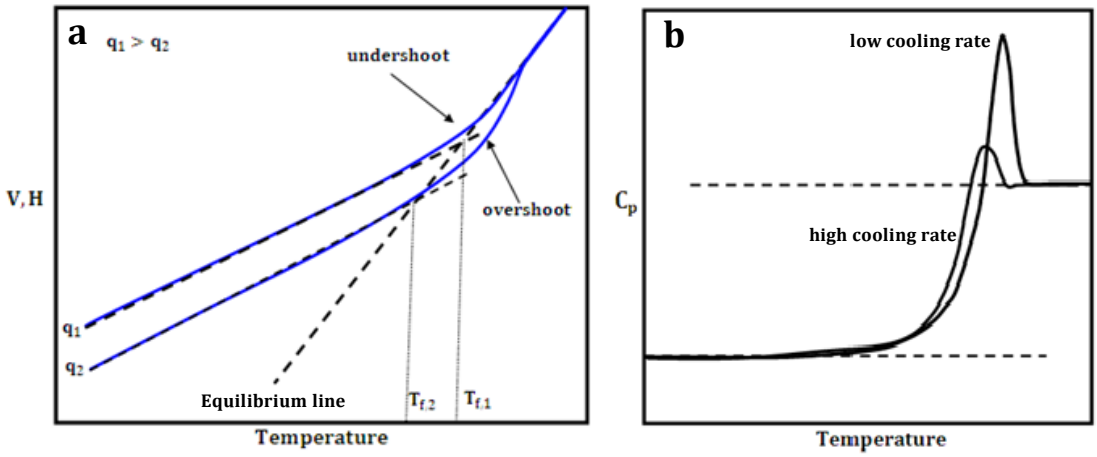

Figure 1.3 a. Specific volume or enthalpy versus temperature at two cooling rates. **b.** The heat capacity vs. temperature at a low cooling rate and a high cooling rate for a constant heating rate.

Limiting fictive temperature (T_f') refers to the temperature at which the glass is unaged.[3,11] Commonly, T_f' is used instead of T_g [12,13]. However, experimentally T_g is about 1 K higher than T_f'.[3]

1.3 Glass Transition Temperature in Confined Systems: Polystyrene Thin Films

1.3.1 Glass Transition Temperature in Supported Polystyrene Films

The first observation of glass transition temperature reduction in polymer films was presented by Keddie *et al.*[14-16] with their work of supported (on Si substrate) polystyrene thin films. The Keddie *et al*.[14-16] work consisted of using ellipsometry to investigate the T_g dependence on the thickness of the supported films. They also considered the molecular weight effects. The thicknesses used in their study ranged from 10 to 200 nm and the molecular weight ranged from 120 kg/mol to 2900 kg/mol. Furthermore, evidence of T_g reductions was observed for cases where the film thickness was below 40 nm.[14-16] However, no molecular weight dependence was observed. Forrest *et al.*[17] also compared the freely standing polystyrene films to PS supported films (sandwiched between two silicon wafers). They also observed that the decrease in T_g was more pronounced in the case of the freely standing than the supported films. Furthermore, the glass transition temperature dependence on thickness gets influenced by not only the thickness but the substrate used in the case of the supported films (at one surface or two surfaces). For supported films, Forrest and Dalnoki-Veress[18] reported a plot which contained a combination of T_g reductions as the film thickness decreases for polystyrene films.[18] Furthermore, the T_g of supported

polymer thin films might be affected by the polymer film free surface and the molecular mobility.

Throughout the years several other studies on polystyrene thin films have been reported, as it is the case of Bäumchen *et al.*[21] their work consisted of polystyrene thin films with thicknesses ranging from 35 to 114 nm and molecular weight of 592 and 1144 kg/mol. For this particular work, they studied the effect of substrate and molecular weight on the T_g – film thickness dependence. The films were annealed at 130 ^oC for 24 hrs. The films were first used as freely standing and then the same films were used as supported films (on Si wafer with the native oxide layer). The temperature dependence was then studied via ellipsometry. It was claimed by Bäumchen *et al.*[21] that the freely standing films had a different T_g dependence than the ones observed on the supported films. The T_g reductions were observed in the freely standing films and not in the supported ones.

Most recently, Glynos *et al.*[22,23] reported studies on linear and star-shaped PS. The star shaped PS used had functionalities of 3, 4, and 8 arms. The film thicknesses ranged from ~20 nm to 225 nm and they were supported on silicon substrates. The films below 50 nm were annealed for 12 hrs, while the films above 50 nm were annealed for 24 hrs at T_g + 40 ^oC. The temperature dependence on the film thickness was studied via angle spectroscopic ellipsometry. Glynos *et al.* [22,23] observed that the 3-arm star PS, and the long 8 arm star PS films show the same T_g dependence on film thickness as that observed on the linear PS. However, the short branched 8-arm star PS films (10 kg/mol per arm) behaved differently having increased T_g as the film

thickness decreased. In the case of the 4 arm star PS films, the T_g dependence on thickness was weaker than the linear and 3 arm star PS films.

1.3.2 Glass Transition Temperature in Freely Standing Polystyrene Films

Freely standing films refer to the films with no substrate (two free surfaces). Early studies on the freely standing polystyrene films can be associated with work presented by Forrest *et al.*[24] From their work it was observed that the molecular weight affected the T_g of the film. For molecular weights below 378 kg/mol, the film behaves like a supported film, while above molecular weight of 378 kg/mol the T_g reduction was more dramatic. Dalkoni-Veress *et al.*[25] performed transmission ellipsometry on freely standing films with six different molecular weights ranging from 575 kg/mol to 9100 kg/mol and thicknesses ranging from 30 nm to 100 nm. They observed T_g reductions for films below 80 nm in thickness.

O'Connell and McKenna studied freely standing polystyrene films by means of a nanobubble inflation method. The nanobubble method consisted of having a small pressure cell with a template with nano-holes.[26-30] The film is positioned onto the template and pressure is applied. By the applied pressure, nano-bubbles are formed and biaxial creep experiments performed. AFM is used to scan the bubbled surface as function of time.[26-30] They observed that the T_g reductions for their freely standing films were stronger than the ones observed in Keddie *et al.*[14] on their supported films. Additionally, for the study of freely standing films, ellipsometry is a common technique for temperature dependence on thickness for polymer films. Some other

earlier results on polystyrene freely standing films where the molecular weight affects the T_g dependence on thickness is the work presented by Pye and Roth[31] by ellipsometry methods. Their conclusions were that low molecular weight PS films behave more like supported films and upon increasing the molecular weight the film T_g reductions become more pronounced, having some agreement with Forrest *et al.* results.[24,25]

1.3.3 Glass Transition Temperature for Films Dewetted on Liquid Substrate

Films dewetted on a liquid substrate have a different T_g – film thickness response from that observed in the freely standing or the supported films. Bodiguel and Fretigny[32-34] studied the viscoelastic properties of thin polystyrene films by liquid (glycerol) dewetting method. They observed that for films with thicknesses as low as 20 nm there was not very much decrease in T_g. However, Wang and McKenna[35,36] expanded the liquid dewetting studies of linear PS thin films by working with films as thin as 4 nm. They observed a decrease in T_g for films below thicknesses of 20 nm.[35,36] The T_g – film thickness response was observed to be similar in behavior to the one presented by Keddie *et al.*[14] for PS films on Si substrate. Furthermore, Lu *et al.*[37] also worked with PS films but floated them on an ionic liquid substrate. Wang and McKenna[35,36] found small differences in the T_g – thickness response for the films dewetted on glycerol or the ionic liquid. However, Lu *et al.*[37] reported there is not a T_g dependence on thickness or molecular weight for a film thicknesses ranging from 6 to 166 nm.

Similarly, other works have shown that not only different experimental techniques[38-41] might affect the T_g of thin films but also the interfacial energy[42], polymer architecture[22,23], annealing conditions[43], among others[44].

1.4 Dynamic Fragility

Dynamic fragility refers to how the relaxation time (τ) or the viscosity (η) changes as the glass transition temperature of the glass forming material gets approached from above T_g.[45-55] The dynamic fragility was greatly explored in the 1980s by Angell.[45] He suggested plotting of the viscosity vs. a dimensionless temperature scale T^*/T. The T^* was referred to be the temperature at which η reaches a value of 10^{12} Pa.s or 10^{11} Pa.s (the latest being a common value for molecular liquids), thereby T^* gets associated to T_g. Different glass-forming materials show different behaviors when the viscosity (or the relaxation time, τ) vs. T_g/T are plotted.[45] Depending on the temperature dependence two behaviors might be observed: strong (Arrhenius behavior)[45-55] or fragile (non-Arrhenius behavior)[45-55].

1.4.1 Measures of Dynamic Fragility

1.4.1.1 Voguel-Fulcher-Tamman Equation (VFT)

The dynamic fragility of many glass-forming materials can be obtained by means of the VFT[6-8] equation (Eq. 1.1). However, not all materials can be adequately described by the VFT form since the behavior of the scaled temperature dependence might be of Arrhenius form.

$$\eta(T) = \eta_o \exp \frac{B}{T - T_\infty} \quad (1.1)$$

where η is the viscosity at temperature T, and η_o, B, and T_∞ are constants.

The dynamic fragility can be defined as follows[45,50,51]

$$m = \frac{1}{T_g} \frac{d \log \eta}{d \left(\frac{1}{T}\right)}\Bigg|_{T=T_g} = \frac{BT_g}{(T_g - T_\infty)^2} \quad (1.2)$$

where fragility is the slope at T_g and T_g is when the log η is equal to 10^{12} Pa.s (or relaxation time $\tau(T_g)$ =100s) as defined by Angell *et al.*[45] The Angell plot shows the shear viscosity data for glass forming liquids that range from fragile (non-Arrhenius) to strong (Arrhenius) behaviors.[45]

1.4.1.2 William-Landel-Ferry Expression (WLF)

The dynamic fragility for polymeric materials can be obtained by means of the WLF[9] expression (Equation 1.3) in instances where the shift factors related to the α-segmental relaxation (rather than the viscosity) with dependence on temperature of glass-forming materials are known.

$$\log a_T = \log \frac{\tau}{\tau_{ref}} = \frac{-C_1 (T - T_g)}{C_2 + T - T_g} \quad (1.3)$$

1.4.1.3 T_g Dependence on Cooling Rate (q)

T_g depends on the cooling rate q, and it has been suggested that the T_g follows an exponential form (Eq. 1.4). By means of this dependence, the dynamic fragility is obtained by using the Arrhenius form of Equation 1.4 by obtaining the slope of the Arrhenius form at T_g. Fragility can be expressed as a comparison of cooling rates q and q_{std} (Eq. 1.5)[52]

$$q = q_o exp\left[-\frac{E_g}{R\,T_g}\right] \qquad (1.4)$$

where q_o is a constant, $E_g$is the activation energy for the structural relaxation, R is the gas constant.

$$\log\left(\frac{q}{q_{std}}\right) = \; m - m\,\frac{T_{f,std}}{T_f} \qquad (1.5)$$

where q_{std}refers to the cooling rate which corresponds to the cooling rate that matches the heating rate used in the DSC scan. $T_{f,std}$ refers to the standard fictive temperature which was obtained by using the same cooling and heating rates.

Therefore, Equation 1.5 shows that the dynamic fragility can be obtained from the slope or intercept of the equation of the line obtained from plotting the logarithm of the reduced cooling rate vs. the reciprocal of the reduced fictive temperature plot. One scenario was the one presented by Wang *et al.*[52] their work consisted of taking into account seven cooling rates ranging from 80 to 0.5 K/min for their determination of the dynamic fragility via DSC measurements. They found that decalin has a dynamic fragility of 145 (Figure 1.4).

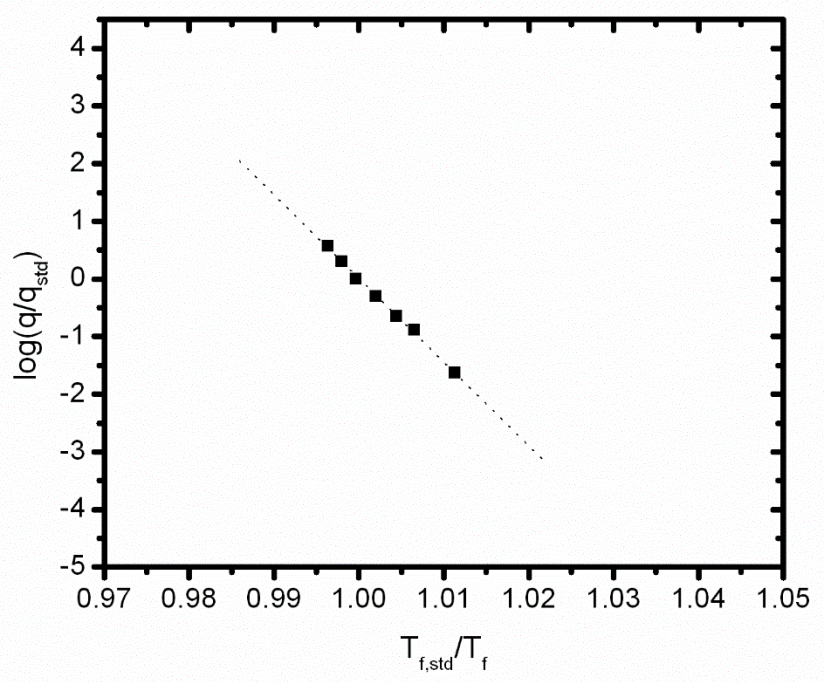

Figure 1.4 Logarithm of the reduced cooling rate vs. the reciprocal of the reduced fictive temperature (reported by Wang *et al.*[52]) of decalin via calorimetric studies for determination of dynamic fragility.

1.5 Purpose of this Work

The current work can be divided into two sections. The first part corresponds to the studies of the glass transition temperature T_g dependence on the film thickness by using a liquid dewetting method. For this particular study, a liquid dewetting method is used to determine the T_g for different polymeric thin films of polystyrene (linear, 3-arm star, and short and long branched 8-arm star PS) with different film thicknesses. The dewetting method is applied either by running the dewetting experiment at a fixed temperature or by applying a temperature step. The difference between the two methods consists on using a limited number of samples. The temperature step dewetting method has the capability of providing the dewetting information that separate tests can provide by only using one sample. The results are

then compared with those of literature data for previous studies of films on liquid substrate, supported films, and freely standing films. The second part corresponds to the study of the dynamic fragility of bulk polymers and lactic acid. Dynamic fragility is obtained by means of calorimetric studies by obtaining the fictive temperature dependence on cooling rate. At the same time, rheological studies are also performed on some of the materials to obtain the dynamic fragility. The current dynamic fragility work was motivated by recent published works[55] that report that some polymers have significantly higher dynamic fragilities than previously reported. This increase in dynamic fragility was attributed to a wash-precipitation treatment on the polymer. The current study compares dynamic fragility results with those previously reported.

CHAPTER II

EXPERIMENTAL TECHNIQUES

2.1 Introduction

In the current investigation three different techniques are used. One technique corresponds to the liquid dewetting technique via a self-built liquid dewetting apparatus along with an already existing liquid dewetting apparatus in our Texas Tech University lab. This technique is used to obtain the glass transition temperature (T_g) dependence on the thickness of polymeric thin films.

The second technique refers to the thermal methods. The calorimetric technique helped to obtain the glass transition temperature (fictive temperature was used in the study) dependence on cooling rate. Obtaining this T_f - q dependence helped to later determine the dynamic fragility of small molecules and bulk polymeric glass forming materials. This technique was achieved by using differential scanning calorimetries (DSCs): Perkin-Elmer DSC-7, Mettler Toledo DSC 823 and Mettler Toledo DSC1.

The third technique corresponds to rheological studies. The studies were performed via an ARES rheometer from TA from where zero shear viscosity[56] and dynamic frequency sweep measurements[57] were performed with the aim of obtaining the dynamic fragility.

2.2 Instruments

2.2.1 Existing Liquid Dewetting Apparatus in our Texas Tech University Lab

The original idea of a liquid dewetting apparatus is attributed to Bodiguel and Fretigny[32-34]. Later Wang and McKenna[35,36] replicated this Bodiguel and Fretigny[32-34] liquid dewetting apparatus (Figure 2.1) at Texas Tech University. Some modifications to the original apparatus were incorporated. These modifications included adding a light ring source to the 10 x optical lens that allowed enhancing the contrast and better identifying the edge of the floating polymeric film. The lens is used in conjunction with a CCD camera (Fire-i 701b, Unibrain Inc.) which captures the images of the film during the experimental time once the film is floated onto the preheated liquid bath. Another modification included adding a needle-like pin to the bath to be able to anchor the floated film, thereby keeping the film within camera view.

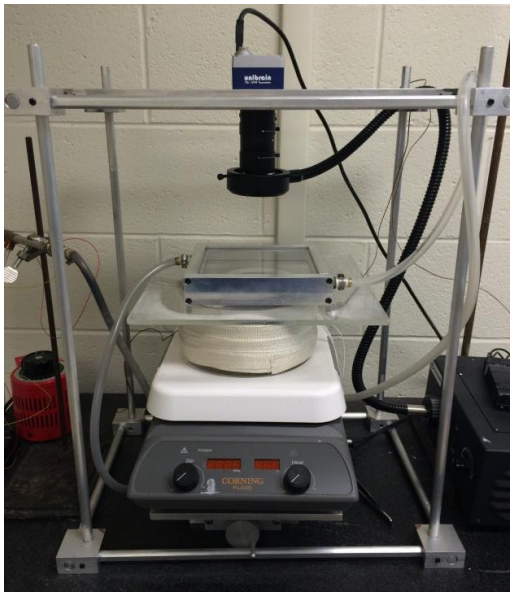

Figure 2.1 Image of built dewetting apparatus at Texas Tech University.

2.2.2 Self-Built Liquid Dewetting Apparatus in our Texas Tech University Lab

The self-built dewetting apparatus is similar in idea to the one used by Bodiguel and Fretigny[32-34] and Wang and McKenna[35,36]. However, modifications were applied to the new dewetting apparatus (Figure 2.2). The self-built dewetting apparatus consists of a double-walled beaker that serves as the bath-container for the liquid substrate. Air heaters (compressed air passing through them) are used to pass heated air through the walls to heat the beaker, as a result heating the glycerol. The inner double walled section of the beaker is painted with a high-temperature black enamel to allow for contrast enhancement then allowing the edge of the floating film to be seen. The temperature inside the bath is then controlled by using a relay, a thermocouple, and a variable AC voltage transformer. The achieved temperature control is of ± 0.3 ºC. A thin glass needle-like pin is used to keep the thin polymeric floated film within camera view. The images are capture by a CCD camera (Fire-i 721b, Unibrain Inc.) with a 10 x optical lens. The advantage of the current setup is that the desired experimental temperature is achieved in a more rapid manner.

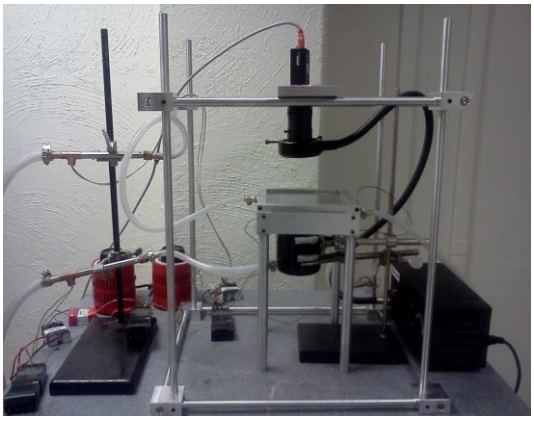

Figure 2.2 Image of self-built dewetting apparatus at Texas Tech University.

2.2.3 Atomic Force Microscopy (AFM)

A Quesant USPM (Universal Scanning Probe Microscope, Figure 2.3) was used on tapping mode and using NSC16 silicon nitride tips to measure the initial film thickness of the polymeric thin films (films were supported on Si wafers) and to assure that the annealing conditions used did not dewet the films.[41]

Figure 2.3 Atomic Force Microscope with 40 μm head.

2.2.4 Rame and Hart Goniometer

A goniometer (Model 100-00 from Rame and Hart, Inc.) was used to obtain the contact angle between the polystyrene samples and the liquid substrate for the dewetting experiment.

2.2.5 Differential Scanning Calorimetry (DSC)

A Mettler Toledo DSC 823 and a Perkin-Elmer DSC-7 were used to help determine the limiting fictive temperature (T_f') of the linear, branched star polystyrenes, polysulfone (PSF), polycarbonate (PC) and polyvinyl chloride (PVC). The limiting fictive temperature was calculated by using the Moynihan's area matching method.[13] The DSC-7 was used to determine the fictive temperature (T_f) dependence on cooling rate of PSF, PC, and PVC. Calibrations were performed by using standard calibration samples of indium and tin. The calibrations were performed at cooling and heating rates of 10 or 20 ^{o}C/min. Al pans were used and sample masses for the polystyrene samples were around ~ 4 to 6 mg. In the case of PSF, PC, and PVC, sample masses of 2, 4, and 6 mg were used per polymer.

A Mettler Toledo DSC1 was used to study the fictive temperature dependence on cooling rate for D,L-lactic acid and D-lactic acid.

2.2.6 ARES Rheometer

ARES rheometer from TA was used to do zero shear viscosity and dynamic measurements.

2.3 Experimental Techniques

2.3.1 Liquid Dewetting Method

2.3.1.1 Liquid Substrate Determination

Previous studies from Bodiguel and Fretigny[32-34] and Wang and McKenna[35,36] have shown that glycerol can be used as a liquid substrate for polystyrene samples. Glycerol does not plasticize the polystyrene films and has a high boiling point of 290 ^{o}C.[32-35] It was also investigated by Wang and McKenna[35,36] that glycerol and polystyrene thin films under different conditions and temperatures does not affect nor plasticize the films. Another important factor for choosing a suitable liquid substrate is to have a negative spreading parameter between the film and the chosen liquid substrate. The negative spreading parameter allows for the film to dewet from the substrate instead of wetting from the substrate.[32-36]

Furthermore, the Rame-Hart Goniometer was used to determine the contact angle between polystyrene and the liquid substrate (glycerol). Consequently, the spreading parameter between the polymer and the liquid substrate was obtained. First, the surface energies of the polystyrene samples were determined by using two liquids having different polarities (diiodomethane and water). Furthermore, the dispersive and non-dispersive components of the surface energy of the polymer were calculated after obtaining the contact angle obtained from the polymer and the liquid. A CCD camera and ImageJ are used to capture the image of the drop and to measure the contact angle, respectively[56]. The surface energy of the polymer ($\gamma_{polymer}$) was obtained as follows[57-59]

$$\gamma_{polymer} = \gamma^{d}_{polymer} + \gamma^{p}_{polymer} \qquad (2.1)$$

where the superscript *d* denotes the dispersive interaction of the surface energy and *p* denotes the non-dispersive interaction.

In terms of contact angles the surface energy of the polymer can be denoted as[60,61]

$$\gamma_1 (1 + cos\theta_1)/2 = \left(\gamma^{d}_{polymer}\, \gamma^{d}_{1}\right)^{\frac{1}{2}} + \left(\gamma^{p}_{polymer}\, \gamma^{p}_{1}\right)^{\frac{1}{2}} \qquad (2.2)$$

$$\gamma_2 (1 + cos\theta_2)/2 = \left(\gamma^{d}_{polymer}\, \gamma^{d}_{2}\right)^{\frac{1}{2}} + \left(\gamma^{p}_{polymer}\, \gamma^{p}_{2}\right)^{\frac{1}{2}} \qquad (2.3)$$

where the subscripts 1 or 2 refer to either diiodomethane or water.

Table 1.1. Surface energy values for diiodomethane and water (HPLC grade).[59]

Solvent	***γ (mJ/m²)***	***γ^d (mN/m)***	***γ^p (mN/m)***
Diiodomethane (>99%)	50.8	50.4	0.38
Water (HPLC grade)	72.8	21.8	51.0

Furthermore, after obtaining the surface tension of the polymer and the contact angle between the polymer and the glycerol, the interfacial energy of the polymer and glycerol was obtained (Equation 2.4) and the spreading parameter (S) value between the polymer and glycerol calculated (Equation 2.5).[32-36]

$$0 = \gamma_p - \gamma_{pl} - \gamma_l cos\theta \qquad (2.4)$$

$$S = \gamma_l - \gamma_{pl} - \gamma_p \qquad (2.5)$$

where γ_p is the interfacial energy of the polymer and the air, γ_{pl} is the interfacial energy between the polymer and the liquid, and γ_l the interfacial energy of the liquid and air. In order for the films to dewet the spreading parameter needs to be negative.

In the current liquid dewetting study, linear polystyrene has a surface tension of 40.1 mN/m[32-34], 3 arm star PS has a surface tension of 46.7 mN/m, and 8 arm star PS with 45.5 mN/m. However, there have been other reports that suggest that the surface tension of linear polystyrene might be 33 mN/m. The surface tension of 33 mN/m was reported by Kwok and Neumann[62] from a compilation of results of PS on 34 different substrates. However, when calculating the surface tension, we found it in the range previously presented by Bodiguel and Fretigny.[32-34] The spreading parameter for the linear polystyrene samples on glycerol is -5 mN/m and those of the 3 arm star PS and 8 arm star PS on glycerol are -13 mN/m and -11 mN/m, respectively.

2.3.1.2 Initial Thickness Determination for the Polymeric Thin Films

Atomic force microscope (AFM, Quesant USPM) was used to determine initial thickness of the samples used for the dewetting experiments. The original sample was cut into four equal squares. The film from one of the pieces (mica with the annealed sample) was floated onto water then transferred onto Si wafer and allowed to dry on a dessicator. The film was then marked with three lines by using a razor blade. The film thickness of the PS sample was then obtained by using the AFM in tapping mode (NSC16 tip) and thickness measurement method developed in the lab.[28] The scans were made in at least nine different regions where the lines were made, and the average of the nine obtained thicknesses was assigned to be the initial film thickness of the sample.

2.3.1.3 Liquid Dewetting Temperature-Step Method

The temperature-step dewetting method consists on floating the polymeric thin film onto the preheated glycerol. The dewetting experiment starts and the film starts dewetting. When the dewetting ceases, meaning that the film stops dewetting (stops shrinking), the film reaches a thickness plateau. Without removing the film, the temperature gets increased to the new desired temperature. The new temperature is reached within 5 minutes. The final thickness of the previous run becomes the initial thickness of the consecutive run. Approximately six temperature steps are possible by using this dewetting technique. Thereby, the number of samples used gets minimized and the overall experimental time reduced since the loading and unloading of the samples are prevented.

The instantaneous stress is constantly changing as the instantaneous thickness increases with time. As mentioned, during the dewetting experiment the film (with initial known thickness h_o) shrinks in a homothetic way while the thickness increases with time h(t). Furthermore, in Figure 2.4 the interpretation of the T_g has been taken to be the temperature at which the film stops dewetting, i.e. reaching a thickness plateau (vitrification at T_g) with time.

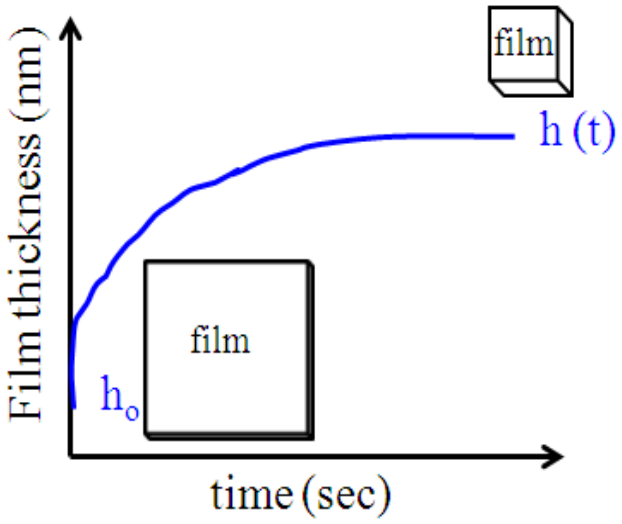

Figure 2.4 Illustration of how the thickness – dewetting behavior occurs. The thickness increases from initial thickness h_o to a final thickness h(t) when it reaches a thickness plateau.

2.3.2 Calorimetric Methods

2.3.2.1 Fictive Temperature Determination by Moynihan's Area Matching Method

Wang *et al.*[52] determined the dynamic fragility (*m*) of polymers and other materials by means of calorimetric studies. DSC was used to obtain the fictive temperature T_f at different cooling rates and at a constant heating rate. The limiting fictive temperature and fictive temperature are found by using the Moynihan's area matching method[13]

$$\int_{T_f'}^{T \gg T_g} (C_{pl} - C_{pg}) dT = \int_{T \ll T_g}^{T \gg T_g} (C_p - C_{pg})\, dT \qquad (2.5)$$

where C_{pl} and C_{pg} are the liquid and glassy state heat capacities, respectively. C_p is the heat capacity of the sample at T_f. Furthermore, it has been shown that *m* can be

obtained from the exponential response of the T_g dependence on the cooling rate *q*. However, T_g can only be properly obtained on cooling. Therefore T_f is used instead.[63] Figure 2.5 shows the DSC heating scan. The lines correspond to the extrapolated liquid (blue) and glassy (red) lines, respectively. The dashed vertical line corresponds to the obtained fictive temperature at which the area I and II are equal as per the Moynihan's area matching method.[13]

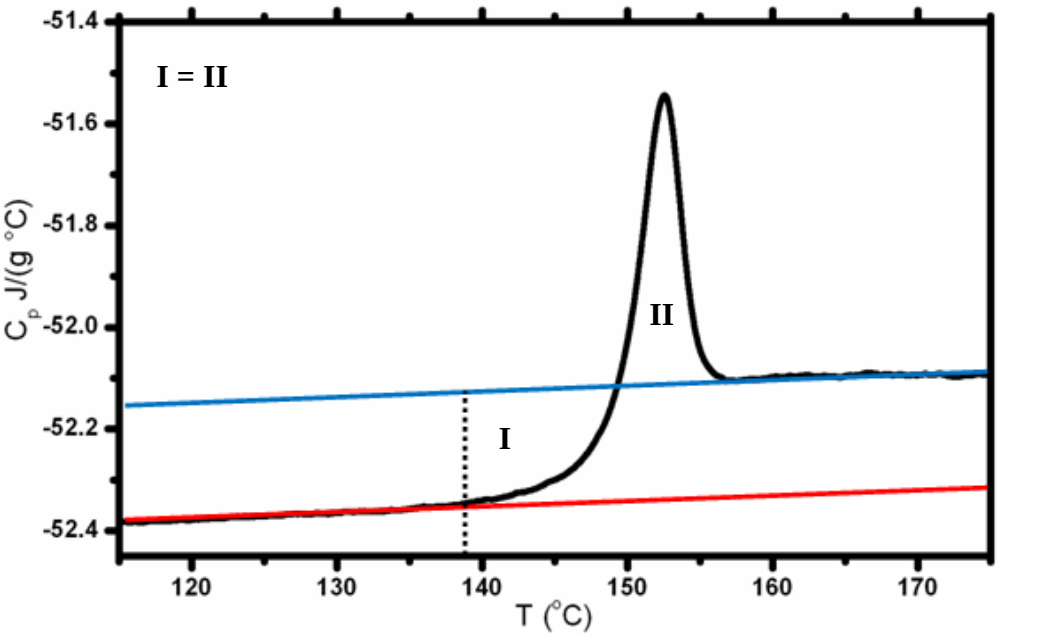

Figure 2.5 DSC scan curve. Extrapolated lines for the glassy (red) and liquid (blue) are shown.

2.3.3 Rheology Methods

2.3.3.1 D,L-Lactic Acid

The dynamic fragility of the D,L-lactic acid can be obtained by obtaining the zero shear viscosity by using the ARES rheometer of the lactic acid by using a parallel plate geometry with platens 8 and 25 mm in diameter.

2.3.3.2 Polysulfone (PSF)

In the case of the as-received and the wash-precipitated PSF, the dynamic fragility was obtained by doing dynamic frequency sweep measurements using ARES rheometer. Disk-like PSF samples were required to run the experiment. PSF samples were prepared by using a hydraulic platen press. The samples were molded while maintained under vacuum by using an oven bag to avoid air voids within the sample. The molded time was of 2 hrs at T_g + 35 ^oC. The experimental temperatures ranged from T_g + 1 °C to T_g + 55 °C, and when the temperatures were in the range below T_g + 5 °C the Struik protocol was followed.[64] Compliance corrections to all data were applied following the Hutcheson and McKenna method.[65]

CHAPTER III

TEMPERATURE-STEP LIQUID DEWETTING TECHNIQUE FOR TG DETERMINATION OF THIN POLYMER FILMS

3.1 Introduction

The liquid dewetting method consists of the polymer film on the appropriate liquid shrinking in a homothetic manner when the temperature is above the T_g of the specific thickness film. The film stops dewetting (thickness stops increasing and reaches a thickness plateau) when the experimental temperature approaches the T_g of the film due to the vitrification of the polymer. Thus, the experimental temperature becomes the T_g of the polymer at a specific film thickness. Furthermore, the temperature step dewetting method consists of applying a sequence of temperature steps during the dewetting experiment. Therefore, allowing the determination of multiple T_g vs. film thicknesses from a single thin film sample having initial thickness h_o.

Studies of dewetting of polystyrene thin films on glycerol previously reported by Bodiguel and Fretigny[32-34] and Wang and McKenna[35,36] have shown either no change in T_g relative to the bulk T_g value for thicknesses above approximately 25 nm or T_g reductions for thicknesses below approximately 25 nm. Additionally, an interfacial influence on the dewetting behavior was observed for PS thin films as evidenced by differences in response of films being dewet from glycerol or from an ionic liquid.[37] Furthermore, the observed T_g reductions in the dewetting experiments have been reported to be more similar to those observed for polystyrene on silicon

substrates as presented by Keddie *et al.*[14] than those of freely standing polystyrene films. Nonetheless, the T_g depressions obtained from the dewetting method differ from both those obtained from supported and those obtained from freestanding films.

In addition, literature reports from Glynos *et al.*[22,23] suggest that the molecular architecture (e.g., star branched vs. linear polymers) impacts the T_g-thickness behavior of PS films. Glynos *et al.*[22,23] reported that a short chain branched 8-arm star PS film shows an increase in T_g (film thickness < 50 nm) rather than a T_g depression as in linear or long branched 3-arm star PS films. In the current study, a temperature - step dewetting method was used to investigate the dewetting behaviors of linear, 3-arm star, and 8-arm star PS. The T_g reductions are compared to those previously reported from the dewetting method at fixed temperatures and the temperature step dewetting method on linear polystyrene films. The study is followed by a comparison of the current results with those previously reported for liquid dewetting, freely standing films, supported films, and the results reported by Glynos *et al.*[22,23] on the role of the polymer architecture in the T_g - thickness response.

3.2 Experimental Methods

3.2.1 Materials

Linear polystyrene (PS) (M_w = 9.8 x 10^5 g/mol with PDI = 1.03). Additionally, 3 arm star PS (M_n per branch of 1.10 x 10^5 g/mol with PDI = 1.07), short branched 8 arm star PS (M_n per branch of 9.8 x 10^3 g/mol with PDI = 1.04), and long branched 8 arm star PS (M_n per branch of 57 x 10^3 g/mol with PDI = 1.08 from Dr.

Dimitris Vlassopoulos). The limiting fictive temperatures (T_f) were found to be 101.4 °C, 100.4 °C, 85.5 °C, and 90 °C respectively (DSC on heating at 10 °C/min after cooling at 10 °C/min).

3.2.2 Sample Preparation

3.2.2.1 Sample Preparation: Thin Films

Linear PS and branched star PS in toluene solutions with weight fractions ranging from 0.15 to 3% were used to prepare different film thicknesses. The polymeric solutions were spin coated onto freshly cleaved mica sheets at room temperature at 2000 rpm. The original sample size was approximately 25 x 25 mm. Samples were annealed at T_g + 20 ^oC for 30 min. The 30 min annealing time was chosen to avoid dewetting of the film from the substrate.

3.3 Data Analysis

3.3.1 Theoretical Analysis

The overall idea behind the dewetting method is that the polymeric film dewets (shrinks in a homothetic way) while the thickness increases with time. In order for the film to dewet, the spreading parameter between the polymeric film and the substrate (glycerol) needs to be negative.[32-36] The idea is to start with a thin film with known h_o on preheated glycerol with a temperature below the bulk T_g. Therefore, the film does not dewet (does not shrink) because the forces from the spreading parameter

are too low to significantly affect or deform the polymer film. Upon increasing the temperature of the bath, if the temperature is still too low then the polymer film will remain glassy (non-deformed). However, if the temperature is above the reduced T_g of the film, the film will start to shrink. As the film thickness increases, the T_g also goes up, and when the T_g is again above the T_g of the new film thickness the film stops dewetting. Furthermore, the strain can be obtained by calculating the changes on the film area. The Hencky strain equation is used to calculate for the strain response.[32-36] The instantaneous film thickness is then determined. On the contrary, if the spreading parameter between the film and glycerol is positive, the film would just get thinner and thinner once the experimental temperature is above T_g.

3.3.2 Results and Discussion

3.3.2.1 Polymer Film Thickness Effect on T_g: Dewetting at Fixed Temperature

In the current work, liquid dewetting experiments were performed on thin polystyrene films. Dewetting experiments were first performed on linear polystyrene films. It was observed (Figure 3.1) that a film with initial thickness of 6 nm dewets at different rates depending on the experimental temperature used. In the case of 60ºC, the film does not dewet (does not deform) after an experimental time of 20 hrs. However, when a new film with same initial thickness is used at a temperature of 65ºC, dewetting of the 6 nm film is observed. The film starts to shrink and the thickness increases with time, though the thickness increases no more than 0.5 nm. It is also observed that the 6 nm films dewetted towards a thickness plateau that

depended on the experimental temperature used. For the films with greater initial thickness as in the case of the 20 and 24 nm films dewetting at a fixed temperature of 100 ^{o}C, the final thickness for both cases tends towards an approximate thickness of around 34 nm. Furthermore, the bulk T_g for the linear polystyrene is 101.4 ^{o}C, meaning the dewetting at 100 ^{o}C with final thickness of 34 nm would be a good approximation of the thickness at which the material should have bulk-like characteristics. The final thickness at the end of every experimental temperature (when the thickness reaches a plateau) is determined by taking the derivative of the thickness with time (dh/dt). The thickness plateau (or the thickness at vitrification) is achieved when the dh/dt is less than 3 x 10^{-5} nm/s as suggested by Wang and McKenna.[36] Figure 3.2 shows the dh/dt for the film with initial thickness of 6 nm at experimental temperature of 85 ^{o}C (data from Figure 3.1).

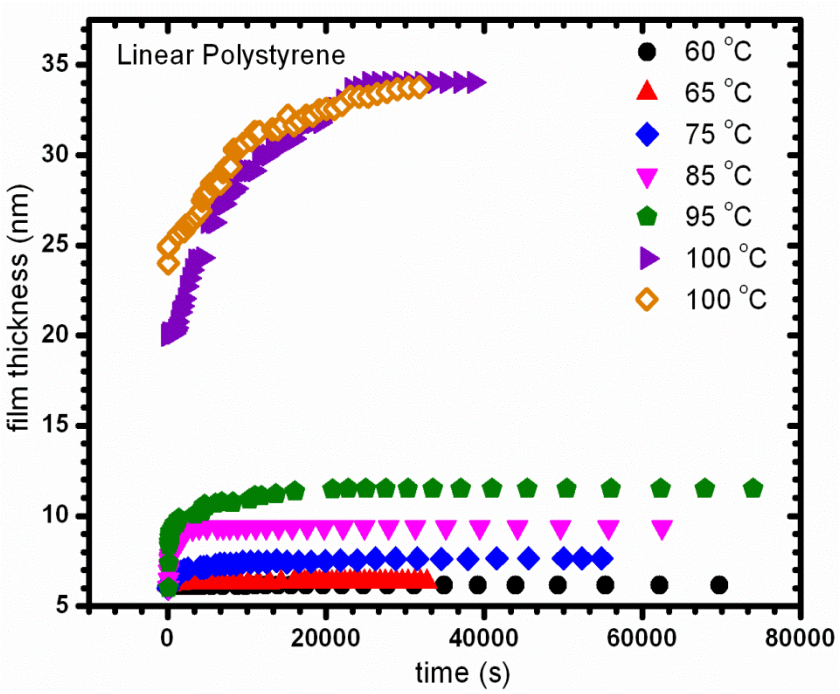

Figure 3.1 The 6 nm linear PS film dewetting from glycerol at fixed temperatures.

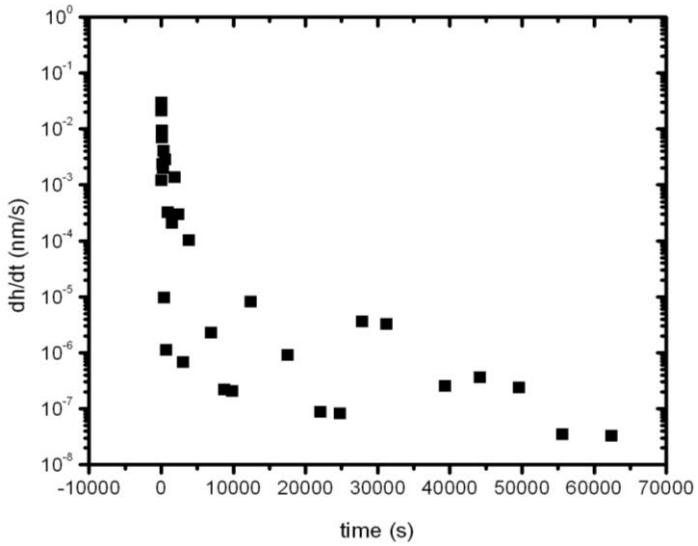

Figure 3.2 The derivative (dh/dt) of the experimental data for the 6 nm linear PS film that dewetted at 85 ^{o}C.

3.3.2.2 Temperature-Step Method and the Effect of Polymer Architecture on T_g

The intent of this work is to be able to use the temperature-step dewetting method to obtain the T_g – thickness dependence of polymer films. The idea behind the temperature-step dewetting method is to use one single film and dewet it under consecutive temperature steps. For that reason, we first start by introducing the idea of the T-step method. The data from Figure 3.1 is plotted as a continuous dewetting experiment to give a 'reference' curve as shown in Figure 3.3. Then Figure 3.3 looks like a 'temperature-step' experiment. The plot is created by starting with the film of 6 nm at temperature of 60 ^{o}C, followed by the experimental data for dewetting experiment at 65 ^{o}C. The same is done for the runs at 75, 85, and 95 ^{o}C (only approximately the first 8 hrs of the experiment are plotted in all cases).

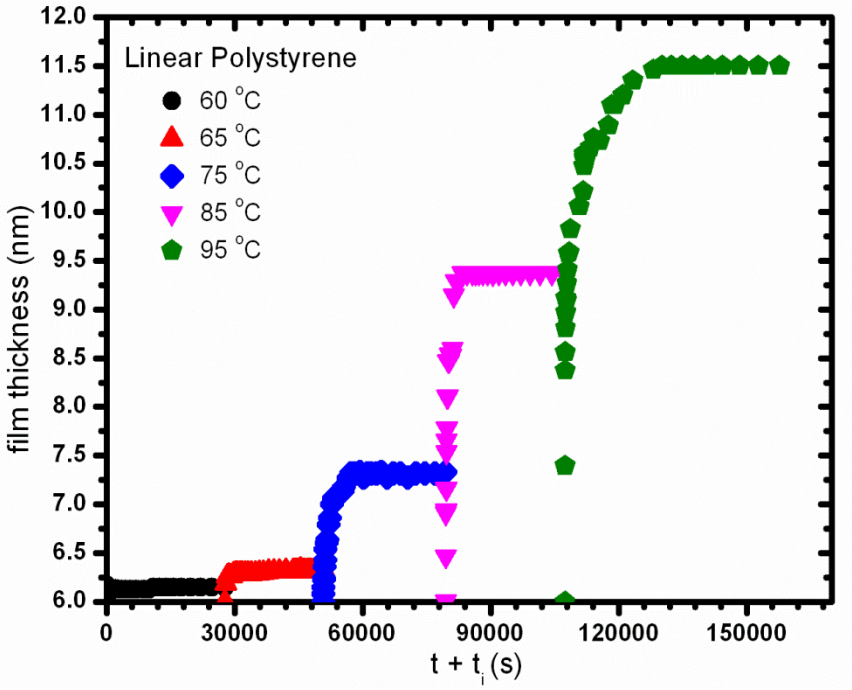

Figure 3.3 The "reference" curve for five separate 6 nm linear PS samples at fixed temperatures.

Figure 3.3 is later used to compare the results of the thickness plateaus obtained from dewetting a single film at a fixed temperature with those thickness plateaus obtained from the temperature-step dewetting method. The T_g-thickness behaviors of different polystyrene samples with different architectures were investigated using the liquid dewetting method. One of the polystyrene architectures is the 3 arm star polystyrene; the films had initial thickness of 6 nm. Therefore, the film dewets upon contact with the heated glycerol. At a particular point the film will cease to dewet. The T_g of the film is then determined as the experimental temperature at which the film stops dewetting. The thickness when the film stops dewetting (when the film reaches a plateau) is the thickness at which the T_g is equal to the experimental temperature.

For the 3 arm star polystyrene film with initial thickness of 6 nm the experimental time per dewetting run was 8 hrs, sufficient time such that the thickness plateaus are clearly observed. After 8 hrs, the temperature was increased and the dewetting reinitiated with the new initial film thickness (which is the final thickness of the previous dewetting run). At the end of the temperature-step dewetting run, a new film thickness is obtained. Figure 3.4 shows the linear PS and the 3 arm star PS dewetting responses when the films are dewetted under consecutive temperature steps. The initial film thickness for all cases was 6 nm. Along with the data from the temperature-step dewetting method, the data of the shifted ('reference') dewetting response for several films which were dewetted at fixed temperatures (Figure 3.3) are also presented in Figure 3.4. It is observed that either by dewetting different films at fixed temperatures or by using one single film and dewetting using the temperature-step method the final thickness is approximately the same.

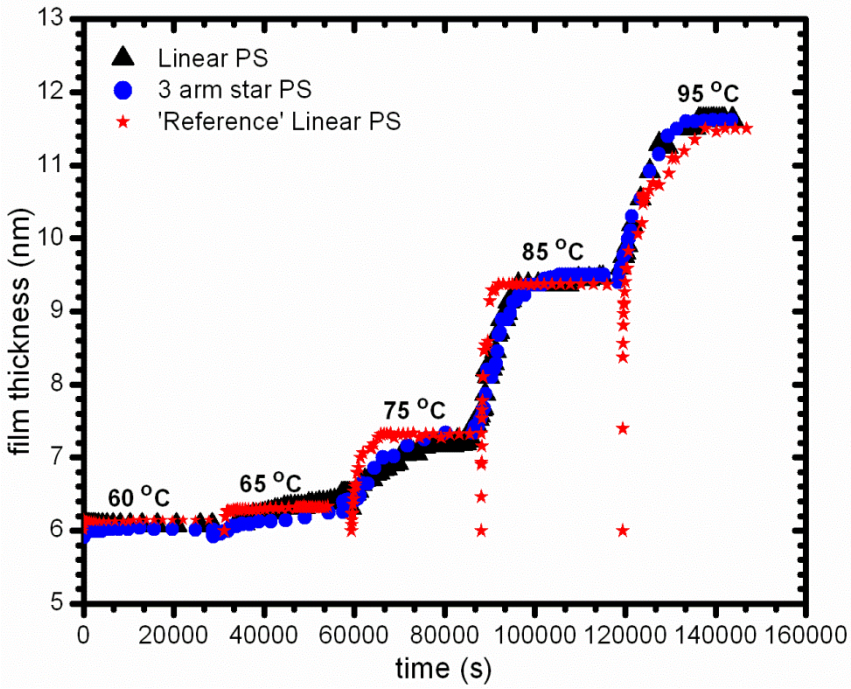

Figure 3.4 The 6 nm linear PS and the 6 nm 3-arm star PS films dewetting from glycerol for successive temperature steps. The data for the "reference" curve for the 6 nm linear PS films dewetted at fixed temperature are also shown.

Figure 3.5 shows an 8 arm star PS film with initial thickness of 6 nm dewetting under consecutive temperature steps. The initial dewetting temperature was 60 ºC for which it was observed that the film did not dewet. Upon increasing the temperature to 65 ºC, the film started to dewet. However, the thickness at the end of the 65 ºC run had increased by no more than 0.3 nm. At the temperature of 75 ºC, the initial thickness of 6.3 nm (which was the final thickness obtained after the dewetting run at 65 ºC) dewets and the thickness plateau is approximately 6.7 nm. The macroscopic T_g of the 8 arm star PS is 85.5 ºC. However, when the film with initial thickness of 6.7 nm is dewetted at 85 ºC, the film reaches a thickness plateau at ~ 8.6 nm meaning that the T_g of the thin film has increased instead of showing a T_g reduction for the linear and the 3 arm star polystyrene.

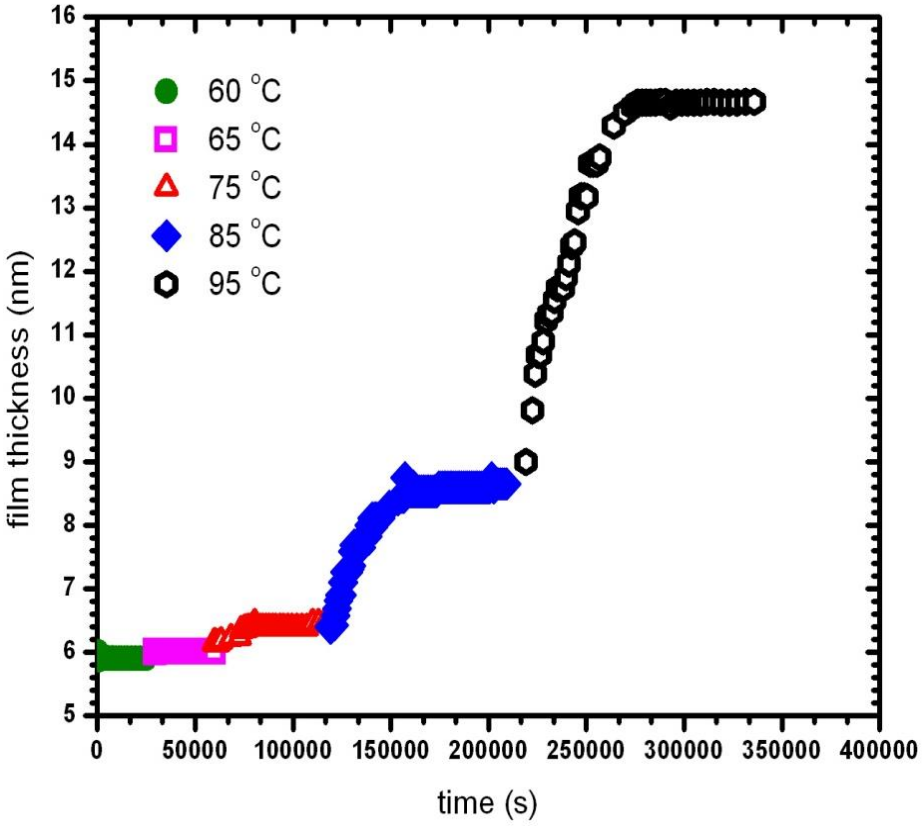

Figure 3.5 The 6 nm 8 arm star PS (with 10000 g/mol arm length) films dewetting from glycerol for successive temperature steps.

Due to the differences in behavior for the 8 arm star PS (10k) with respect to the linear and the 3 arm star PS films. Dewetting experiments on single films were performed with the intent of observing the dewetting behavior at different temperatures with films with same initial thickness. Figure 3.6 shows the dewetting of 8 arm star PS films at some common initial thicknesses but different dewetting temperatures. Four different films with h_o = 6 nm, four films with h_o = 13 nm, two films with h_o = 19 nm, one film with h_o = 14 nm, and one film with h_o = 31 nm were dewetted at fixed temperatures. The dewetting of the 6 nm films at temperatures of 65 and 75 ^oC shows that the film thickness increase is no more than 0.3 nm. For the 6 nm

film at a temperature of 85 ^{o}C, the thickness increases to around 8.1 nm. Furthermore, for the 6 nm film at a temperature of 95 ^{o}C the final thickness is more than twice the initial thickness. Furthermore, the films with initial thicknesses of 13 nm at temperatures of 75 and 85 ^{o}C show no dewetting after around 14 hours of experiment. In the case of the 13 nm film at 95 ^{o}C, the final thickness obtained after 12 hours was 14.3 nm which is within 0.3 nm of the final thickness obtained for the film with initial thickness of 6 nm dewetted at 95 ^{o}C. In the case of 13 nm film dewetting at 105 ^{o}C, the final obtained thickness was of 28 nm which is more than twice the initial thickness of the film.

The final film thicknesses obtained for the dewetting runs at 85 ^{o}C for the films with initial thicknesses of around 6 nm were consistent within 0.3 nm with each other at the end of the run (final thickness of around 8.2 nm). Additionally, the dewetting runs performed at 115 and 120 ^{o}C for films with initial thicknesses of 14, 19, and 32 nm seemed to level off at a thickness around 34 $\pm$ 1nm. The final thicknesses obtained at the end of the runs for the films with h_o = 6 nm are consistent with the thicknesses obtained at the end of the T-step. While there is not a clear explanation at this point, results somewhat are consistent with reports of Glynos *et al.*[22,23] about seeing an increase in T_g for the short branched 8 arm star PS.

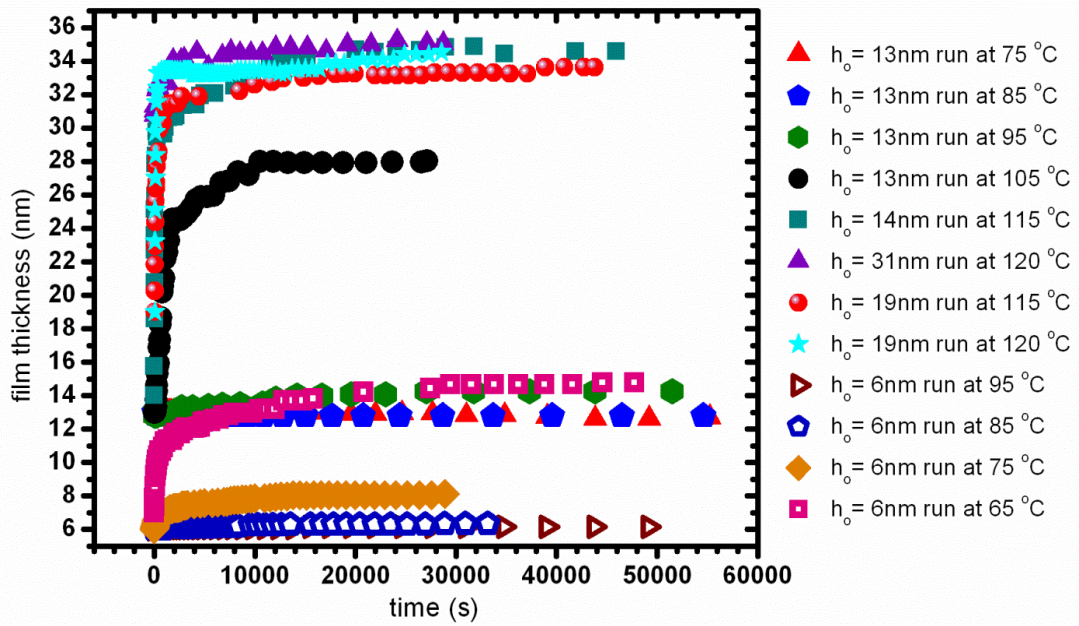

Figure 3.6 The 8-arm star PS (with 10000 g/mol arm length) films dewetting from glycerol at fixed temperatures.

To confirm the findings from the 8 arm star PS (10k) films, dewetting on the long branched star PS (57k) was performed. It was observed (Figure 3.7) that for a film with initial thickness of 6 nm dewetting at a temperature of 65 ^{o}C, the thickness plateau was reached at approximately 6.3 nm. Upon increasing the experimental temperature to 75 ^{o}C (initial film thickness of 6.30 nm) the film started dewetting again and reached a thickness o 6.5 nm. Upon further increase of temperature to 85 ^{o}C (initial thickness of 6.5 nm) a thickness plateau at 7.8 nm was reached. The macroscopic T_g of the 8 arm star PS (57k) is of 90 ^{o}C, and when increasing the temperature from 85 to 90 ^{o}C a thickness plateau at 9.1 nm was reached at the end of the run. The long branched 8 star PS dewetting behavior is similar to the short branched 8 star PS films.

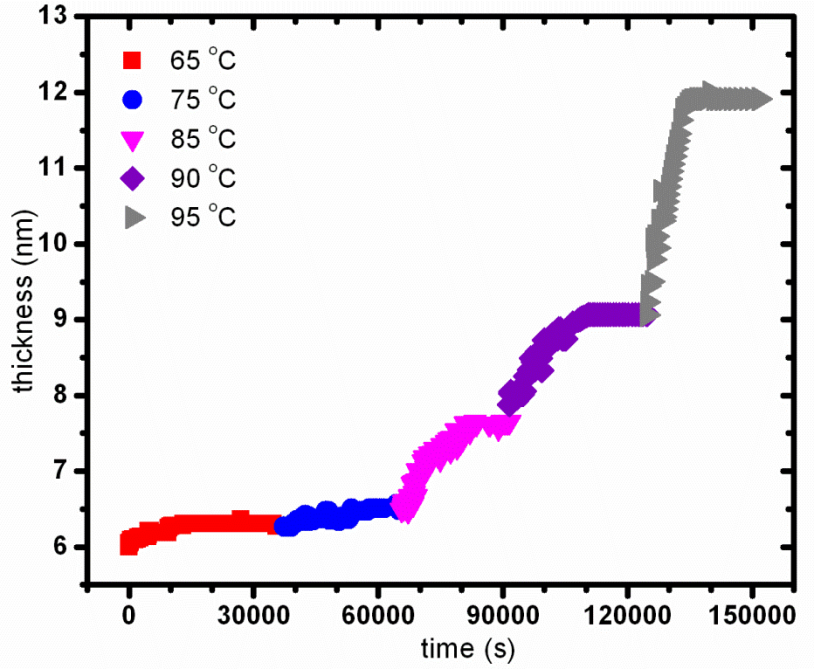

Figure 3.7 The 8-arm star PS (57 kg/mol) film with initial thickness of 6 nm under temperature-step dewetting.

3.3.2.3 Comparison of Current Results with Literature Data

Figure 3.8 shows the current results obtained for the linear, 3-arm and 8-arm PS thin films on glycerol substrate via the temperature-step method alongside previously reported literature ΔT_g values ($\Delta T_g = T_{g,thickness} - T_{g,bulk}$ (K)). The solid line represents the ΔT_g presented by Keddie *et al.*[14] for the PS films on Si substrate. The filled circles represent the ΔT_g presented by O'Connell *et al.*[30] on freestanding PS films via nanobubble inflation method. The T_g reduction results of the liquid dewetting method look closer to the results for supported PS films than the results for freely standing PS films. The T_g reduction results for the linear and 3-arm star PS films are in agreement with previously reported results obtained by Wang and McKenna[36] represented by the open squares (temperature-step method). While there are some variations of the data presented by Wang and McKenna[35] on the PS on glycerol

dewetting at fixed temperature (open triangle) or via the temperature step method (open squares), currrent results seem to follow the trend of Bodiguel and Fretigny[32-34] (open right triangles) results. The filled stars represent the ΔT_g presented by Glynos *et al.*[22-23] for the 8-arm star PS ($M_{w,arm}$ = 10 kg/mol). The results presented by Glynos *et al.* only correspond to film thicknesses ranging from 25 nm to 150 nm. However, these results seem to not follow current ΔT_g values for the 8-arm star PS film. Glynos *et al.*[22,23] reported $\Delta T_g > 0$ and no T_g reductions, while in the current study on the 8-arm star PS a transition from $\Delta T_g < 0$ to $\Delta T_g > 0$ is observed. The thicknesses used in the present work for dewetting were much smaller than those used by Glynos *et al.*[22-23] before T_g reductions are seen compared with supported film T_g reductions. Similarly, T_g reductions are smaller than in supported films. In order to better understand the complex behavior of the 8 arm star PS, results on a sample with M_n = 57 kg/mol per arm are shown. Surprisingly, the results for the long 8 arm star PS are similar to the ones obtained for the short 8 arm star PS.

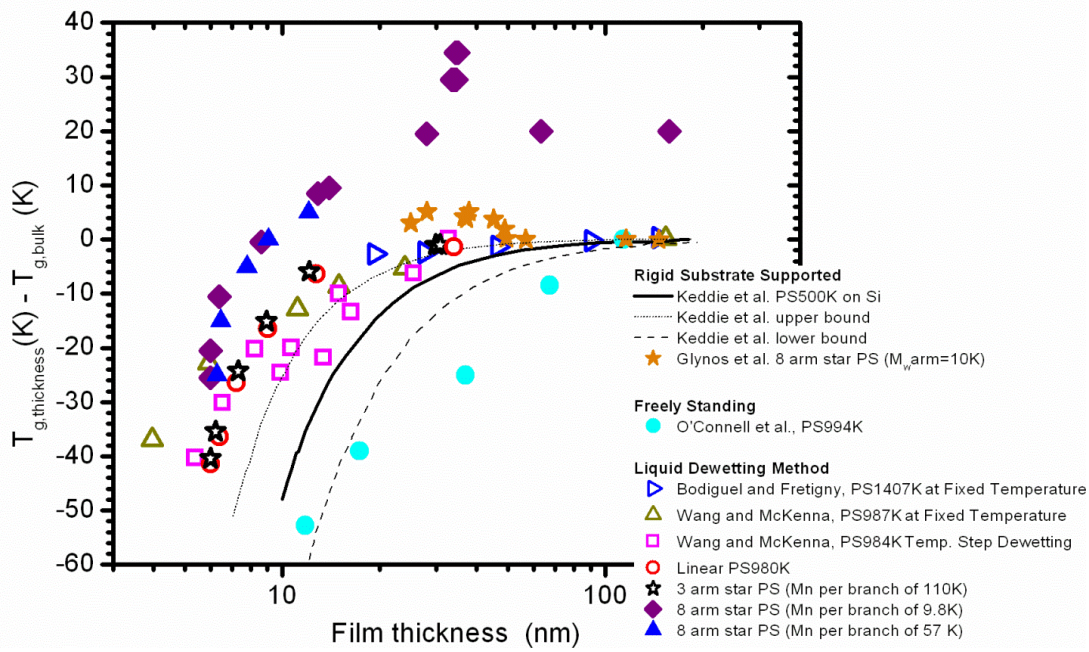

Figure 3.8 Change in T_g as a function of thickness for current PS thin films and literature PS data.

3.4 Conclusions

The liquid dewetting technique was used to obtain the T_g- thickness behavior of linear PS, 3 arm star PS, 8 arm star PS (10k) and 8 arm star PS (57k) films. The dewetting results showed that the linear and the 3 arm star PS films have same T_g – thickness response. However, the 8 arm star PS (10k) and (57k) showed a more complex response. The T_g-thickness response is different from that one observed in previous liquid dewetting measurements reported by Wang and McKenna[35,36] and from the present study, but the results from the 10k and 57k 8-arm star PS have very similar T_g- thickness behaviors with each other. Results then show that not only the thickness affects the T_g of the films, but also the molecular architecture and the molecular weight of the polymer used. The 8 arm star PS films show a non monotonic

response which is much more different from the previous reports on liquid dewetting, freely standing, and supported films.

CHAPTER IV

EXTREMELY FRAGILE GLASS-FORMERS: CALORIMETRIC AND RHEOLOGICAL DETERMINATIONS

4.1 Introduction

Two recent publications from Wang *et al.*[52] and Evans *et al.*[55] are the motivation of the current investigation. In both cases the main focus of the investigation is the dynamic fragility (*m*). Dynamic fragility is commonly used to define the dynamics of the glass-forming material and its dependence on temperature as the glass transition temperature (T_g) is approached from above.[45-52] Therefore, the dynamic fragility is an equilibrium property. The dynamic fragility behavior was greatly studied by Angell in the 1980s.[45] There are two main representations that give Angell plots. There are either the logarithm of the segmental α-relaxation or the viscosity of the glass-forming materials vs. T_g/T. According to the Angell plots[45], the fragile glass former follows a non-Arrhenius behavior[45-52] while the strong glass former follows an Arrhenius[45-52] one. By 2001, McKenna and Huang[49] had compiled the dynamic fragility for 30 polymers and the dynamic fragilities ranged from 23 to 214. The dynamic fragility of 23 corresponds to poly (oxyethylene) and the dynamic fragility of 214 corresponds to polyetherimide.[66-69] The m = 214 for polyetherimide was obtained by combining calorimetric, creep, and dilatometric measurements.[66-69]

The first motivation for the current work arises from a recent publication by Evans *et al.*[55] in which it was reported that as-received and wash-precipitated polymers have different dynamic fragilities. They reported that the wash-precipitation treatment

of the polymers could cause the dynamic fragility to increase to more than twice the literature reported values for the dynamic fragility of the same polymers. Evans *et al.*[55] reported a dynamic fragility of 286 via calorimetric methods for their wash-precipitated polysulfone (PSF) in instances where the dynamic fragility has been reported to be 149 via dielectric relaxation spectroscopy (DRS)[70]. Similarly, Evans *et al.*[55] reported that poly (vinyl chloride) (PVC) via calorimetric studies has *m* of 317 when it had been reported to be 191.[71] Likewise, Evans *et al.*[55] reported that from calorimetric measurements the wash-precipitated polycarbonate (PC) shows a dynamic fragility value of 277 while the as-received PC exhibited a value of 204. However, literature reports for PC fragility have ranged from 119 to 178[72-75]. With the higher values of dynamic fragility obtained from dielectric relaxation spectroscopy and the low values of dynamic fragility via creep experiments. Most recently, Shamim *et al.*[63] reported m = 102 for PC via thermal methods by compiling experiments on conventional DSC (with five cooling rates ranging from 0.1 to 30 K/min) and flash DSC (with nine cooling rates ranging from 0.1 K/s to 1000 K/s).

The second motivation for the current work is based on a recent work by Wang *et al*.[52] where it was speculated that lactic acid should be extremely fragile based on the rapidly changing entropy seen in its Kauzmann plot[76], which expects a strong correlation between the thermodynamic and dynamic fragilities. For example, Wang *et al*.[52] reported the dynamic fragility of decalin with $m = 145$ as a case of extreme fragility for small molecule glass formers and which has a high thermodynamic fragility. However, studies have shown that the correlation between the dynamic and thermodynamic fragilities might not be applicable in all particular cases.[54]

The goal for the current investigation is to test the Wang *et al.*[52] speculation of an extremely high dynamic fragility for D,L-lactic acid and this is studied by both differential scanning calorimetry (DSC) and rheometry. At the same time, we examine the high fragility results from Evans *et al.*[55] by calorimetric measurements for both as-received and wash-precipitated polysulfone (PSF), bisphenol-A-polycarbonate (PC) and poly(vinyl chloride) (PVC). The mentioned polymers are of special interest because Evans *et al.*[55] reported that the wash-precipitation treatment on some polymers can affect the dynamic fragility. The dynamic fragilities are obtained by means of calorimetric studies by studying the cooling rate dependence of the glass transition temperature. However, since T_g can only be appropriately obtained on cooling, the dynamic fragility is obtained by calorimetry via determination of the fictive temperatures (T_f) as a function of cooling rate. Evans *et al.*[55] used small range of cooling rates (5, 10, 20, 40 ^{o}C/min) for determination of dynamic fragility. A broader range of cooling rates (40, 30, 20, 10, 5, 3, 1, 0.5, and 0.3 ^{o}C/min) are used to improve the accuracy of the determined *m*.[52,63] We find that when a small range of high cooling rates is used to determine *m* the value seems to increase compared to results from a broad range of cooling rates that include slower cooling rates.

4.2 Experimental Methods

4.2.1 Materials

Polysulfone (PSF, M_n = 27.6 kg/mol, PDI = 2.7 from Scientific Polymer Products), bisphenol-A-polycarbonate (PC, M_n = 22.4 kg/mol, PDI = 2.1 from Scientific Polymer Products) and poly(vinyl chloride) (PVC, M_n = 63.9 kg/mol, PDI = 2.1 from Scientific Polymer Products). The limiting fictive temperatures were found to be 185, 143.6, and 79.7 °C, respectively. Evans et al. polymers were PSF, (M_n = 20.4 kg/mol, PDI = 3.3 from Scientific Polymer Products), PC (M_n = 17.3 kg/mol, PDI = 1.7 from Scientific Polymer Products) and PVC (M_n = 39.6 kg/mol, PDI = 2.0 from Aldrich). A wash-precipitation treatment following the method described by Evans *et al.*[55] was applied to the as-received PSF, PC, and PVC. In the case of PSF and PC, 1,2-dichloroethane and methanol were used, while for PVC, cyclohexanone and methanol were used.

Gel Permeation Chromatography was used to obtain the molecular weight and polydispersity index of the polymers (PSF, PC, and PVC) used. The RI and UV-vis detectors were used and five different PMMA standard samples were used for the universal calibration.

D,L-lactic acid (Sigma Aldrich, 90% purity) and D-lactic acid (Sigma Aldrich, 93% purity) with limiting fictive temperatures of -80 °C and -65 °C, respectively.

4.2.2 Sample Preparation

Prior to their use PSF, PC, and PVC were dried at 140, 120, and 65 °C for 4 hours, respectively. After drying, the samples were kept in a dessicator. All the DSC samples were prepared under nitrogen atmosphere to avoid moisture absorption. Standard Al pans were used, and the sample weights were of ~ 2, 4, and 6 mg.

PSF samples for rheological studies were prepared by compression molding the PSF by using a platen hydraulic press. The samples were molded at T_g + 35 ^oC for 2 hrs then the molded samples were allowed to slowly cool to room temperature. The molded sample dimensions were of 8 ± 0.05 mm and a thickness of 1.6 ± 0.07 mm.

4.2.3 Instruments

4.2.3.1 Differential Scanning Calorimetry (DSC)

A Mettler Toledo DSC 1 was calibrated on heating with standard samples of octane, indium, and mercury. DSC 1 was used to do the runs for the D,L-lactic acid and the D-lactic acid with nitrogen as the cooling system. The DSC scans were performed from T_g + 30 °C to T_g - 50 °C at various cooling rates ranging from 40 to 0.1 °C/min at a constant heating rate of 10 °C/min.

A Perkin-Elmer DSC-7 was used to perform the calorimetric studies on the polymers. The DSC was calibrated on heating by using standard samples of indium and tin. The calibrations were performed at two different heating rates at 10 ^oC/min and 20 ^oC/min depending on the constant heating rate used (at 10 ^oC/min or 20

^{o}C/min). The DSC scans were performed from T_g + 40 °C to T_g - 50 °C and the cooling rates used were 40, 30, 20, 10, 5, 3, 1, 0.5, and 0.3 ^{o}C/min (nine cooling rates were considered as 'broad range of cooling rates') and two different sets of heating rates were used at 10 or 20 ^{o}C/min.

4.2.3.2 ARES Rheometer

ARES rheometer from TA was used for steady shear viscosity measurements on the D,L-lactic acid and dynamic frequency sweep measurements on the as-received and the wash-precipitated molded PSF samples.

For the D,L-lactic acid, a parallel plate geometry was used with platens of 8 and 25 mm in diameter. The shear rates used range from $1x10^{-5}$ to 1.0×10^{2} s^{-1}, no corrections were required for the viscosity measurements since the study was done in the Newtonian flow regime. The sample was loaded directly onto the bottom platen, the top platen was then slowly lowered down to get in contact with the sample. The gap between the platens was manually adjusted at the different temperatures to keep an optimal sample shape while keeping a positive normal force. The experimental temperatures used were from T_g + 3 °C to T_g + 50 °C. Liquid nitrogen was used to achieve the cold temperatures.

For the PSF samples, the parallel plate geometry was used *w*ith platens of 8 mm in diameter. The sample was loaded onto the bottom platen at room temperature, and then the top platen was then brought in contact with the sample. The initial gap was then recorded. The desired temperature was obtained by modifying the

temperature gradually normally no more than 5 °C with waiting time of 3 min in between temperature changes. Once the desired temperature was reached, a 30 min time for thermal equilibration within the sample was allowed. The experimental temperatures used for the dynamic measurements ranged from T_g + 1 °C to T_g + 40 °C. When working in the range of T_g + 1 °C to T_g + 5 °C, the Struik protocol[64] was followed to assure there was not aging and the equilibrium state of the samples was obtained. The strain used in the dynamic frequency measurements was in the range of 0.01 to 0.5 %. In all particular dynamic data measurements, Hutcheson and McKenna method for compliance correction was applied to the data.[65]

4.3 Data Analysis

4.3.1 Fictive Temperature Determination

Moynihan's area matching method was used to obtain the fictive temperature of the materials used in this study. The fictive temperature (T_f) is obtained instead[77] of the T_g since the T_g can only be appropriately obtained on cooling.[3] The limiting fictive temperature (T_f') can be obtained from the heating scan when heating after cooling at the same rate. The appropriateness of using T_f instead T_g is based on the difference between the T_g and T_f are within 1 K.[3]

$$\int_{T_f'}^{T \gg T_g} (C_{pl} - C_{pg}) dT = \int_{T \ll T_g}^{T \gg T_g} (C_p - C_{pg}) dT \qquad (4.1)$$

where C_{pl} is the liquid state heat capacity and the C_{pg} is the glassy heat capacity, while the C_p is the heat capacity of the sample at T_f'.

4.3.2 Dynamic Fragility Determination from Calorimetric Methods

The dynamic fragility (*m*) can be determined from the plotting the logarithm of the relaxation time (or viscosity) as a function of the inverse of temperature at T_g. In this particular study, T_f is used instead of T_g.[3,63,77]

$$m = \frac{1}{T_g}\frac{d log\, \tau}{d\left(\frac{1}{T}\right)}\Bigg|_{T=T_f} \tag{4.2}$$

where τ is the relaxation time at the fictive temperature T_f.

Wang *et al.*[52] reported that *m* can be obtained from the T_g (this case T_f) dependence on the cooling rate q

$$q = q_o \exp\left[-\frac{E}{RT_g}\right] \tag{4.3}$$

where q_o is a pre-exponential factor, E is the activation energy, R the gas constant.

Eq 4.4 is the representation of eq. 4.3 when expressed as a relation between cooling rates q and q_{std} where q_{std} is the cooling rate that matches the heating rate.[52] Similarly, T_g has been replaced by T_f.

$$\log\left(\frac{q}{q_{std}}\right) = m - m\,\frac{T_{f,std}}{T_f} \tag{4.4}$$

The dynamic fragility is then obtained from the slope of the reduced cooling rate vs. the reciprocal of reduced fictive temperature. The $T_{f,std}$ corresponds to the fictive

temperature (or limiting fictive temperature) obtained when the sample is heated at the same rate at which it was cooled. The q_{std}refers to the cooling rate that matches the heating rate used.[52]

4.3.3 Dynamic Fragility Determination from Rheological Methods

The dynamic fragility can be obtained by using the VFT[6-8] equation

$$\log_{10}\eta = -A' + \frac{B'}{T - T_\infty} \tag{4.5}$$

where η is the zero shear viscosity obtained from the measurements. Here A', B', and T_o are positive constants. From the VFT[6-8] equation the dynamic fragility[52] can be determined by means of

$$m = \frac{B'T_g}{(T_g - T_\infty)^2} \tag{4.6}$$

The dynamic fragility can also be obtained by means of the shift factors used to create the master curve of storage (G') and loss modulus (G'') that incorporate the temperature dependence on the shift factors[62] and the William-Landel-Ferry (WLF)[9,49] expression

$$m = \left.\frac{d\,log\,a_T}{d(\frac{T_g}{T})}\right|_{T=T_g} = \frac{T_g\,C_1^{T_g}}{C_2^{T_g}} \tag{4.7}$$

where $C_1^{T_g}$ and $C_2^{T_g}$ are material parameters at the T_g.[9,49]

$$\log a_T = \frac{-C_1 \left(T - T_g\right)}{C_2 + T - T_g} \tag{4.8}$$

where a_T is the shift factor, C_1 and C_2 are the WLF material parameters.[9,49]

4.4 Results and Discussion

4.4.1 Calorimetry Measurements

4.4.1.1 Lactic Acids

Heating scans for D,L-lactic acid and D-lactic acid are shown (Figure 4.1a and b) at eight different cooling rates ranging from 40 to 0.1 °C/min at a constant heating rate of 10 °C/min. The limiting fictive temperatures of the D,L-lactic acid is -80 °C and for the D-lactic acid is -65 °C.

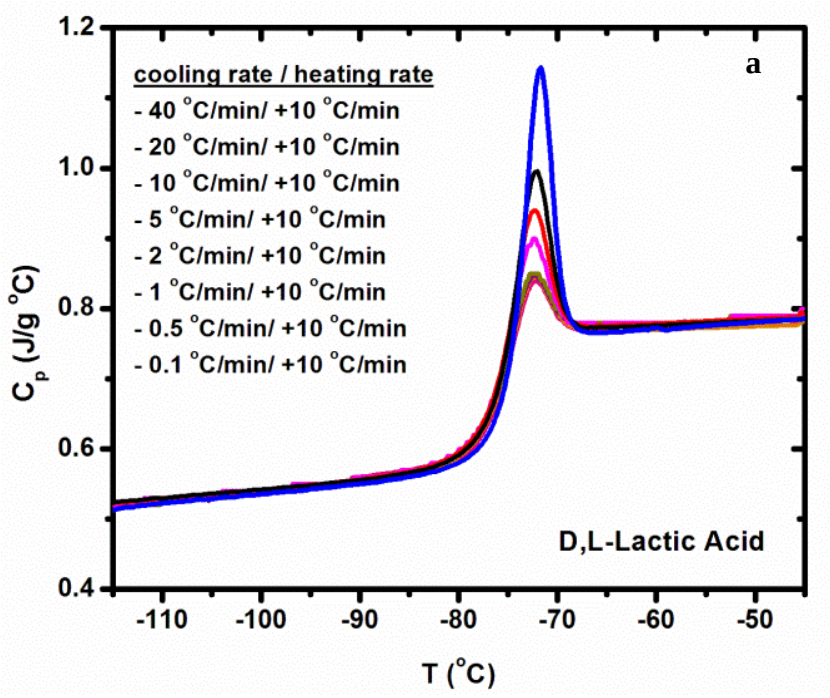

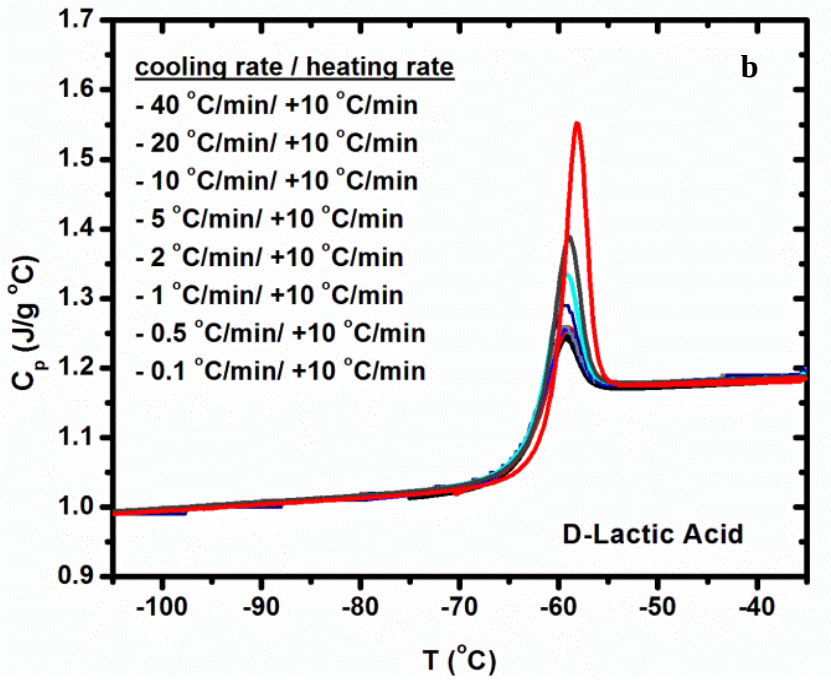

Figure 4.1 (a) Heating scans of the D,L-lactic acid (b) Heating scans of the D-lactic acid. In both cases the DSC scans were at eight different cooling rates at a constant heating rate of 10 ^{o}C/min.

The dynamic fragility was found from the slope of the linear fit of the reduced cooling rate vs. the reciprocal of the reduced fictive temperature.[52] The dynamic fragility of D,L-lactic acid is $m = 80 \pm 2$ and for D-lactic acid is $m = 86 \pm 2$ (Figure 4.2)

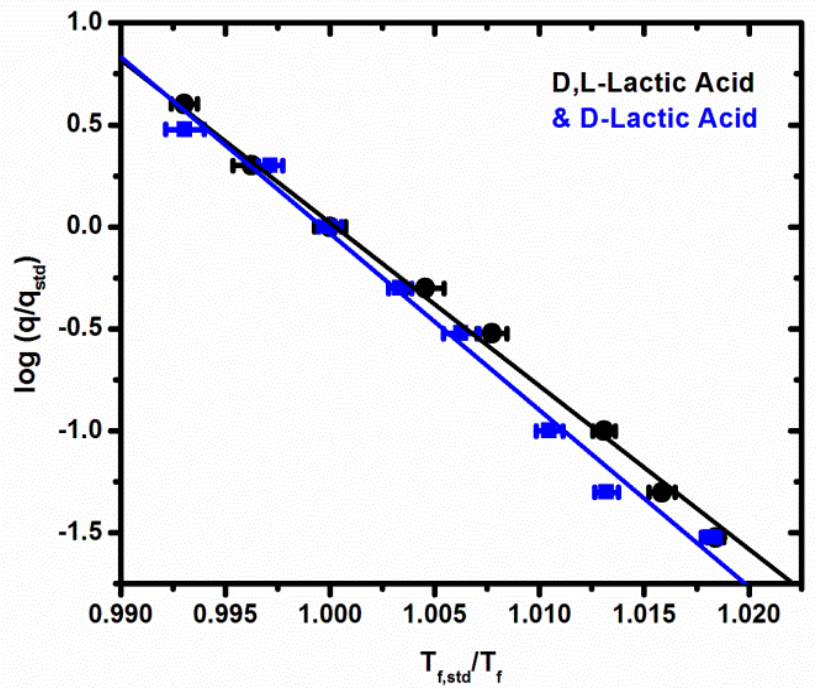

Figure 4.2 The reduced cooling rate vs. the reciprocal of the reduced fictive temperature for the D,L-lactic acid (circles) and the D-lactic acid (squares). The *m* was obtained from the slope or the intercept of the equation of the linear fit.

4.4.1.2 Bulk Polymers

Furthermore, the dynamic fragility for PSF, PC, and PVC was found from the slope of the linear fit of the reduced cooling rate vs. the reciprocal of the reduced fictive temperature. Three different sample masses of 2, 4, and 6 mg were tested to determine if the mass of the sample has any effect on the dynamic fragility results. The range of sample weights used did not affect the fictive temperatures or the dynamic fragility (Figure 4.3).

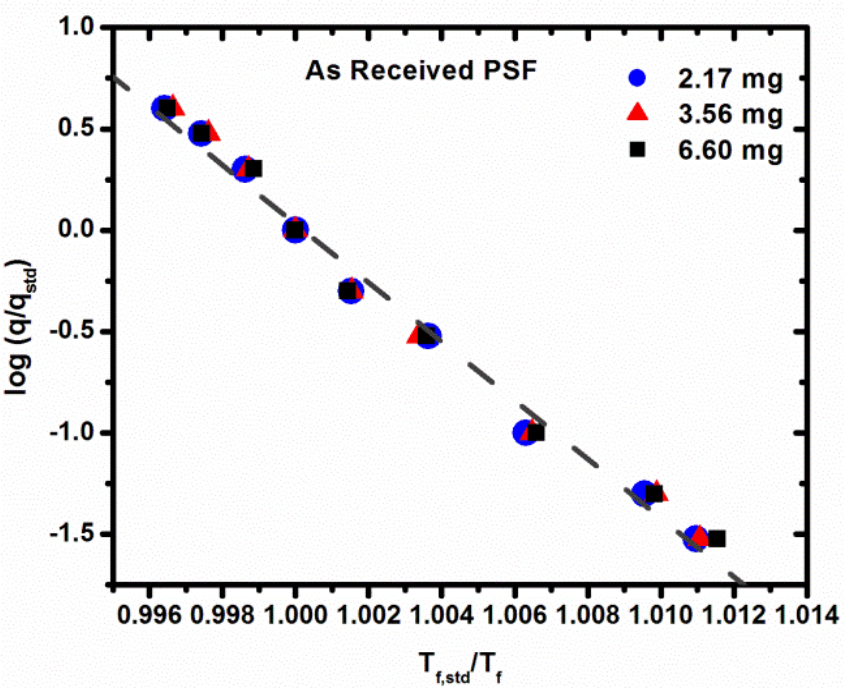

Figure 4.3 Arrhenius plot of the reduced cooling rate vs. the reciprocal of the reduced fictive temperature of three different sample masses for the as-received PSF.

4.4.1.2.1 Polysulfone (PSF)

For the as-received PSF sample (Figure 4.4), the dynamic fragility was found to be 145 ±3 when using a broad range of cooling rates (40 to 0.3 °C/min) at a constant heating rate of 10 °C/min. It was pointed out by Evans *et al.*[55] that the dynamic fragility of wash-precipitated PSF (and other polymers) increases drastically after the treatment. However, in the present study it was found that the dynamic fragility of the wash-precipitated PSF (Figure 4.4 and Figure 4.5) did not change as a result of the treatment. The dynamic fragility of PSF both as-received and after wash-precipitation with the broad range of cooling rates and at constant heating rate of 10 °C/min is m = 145 ± 3.

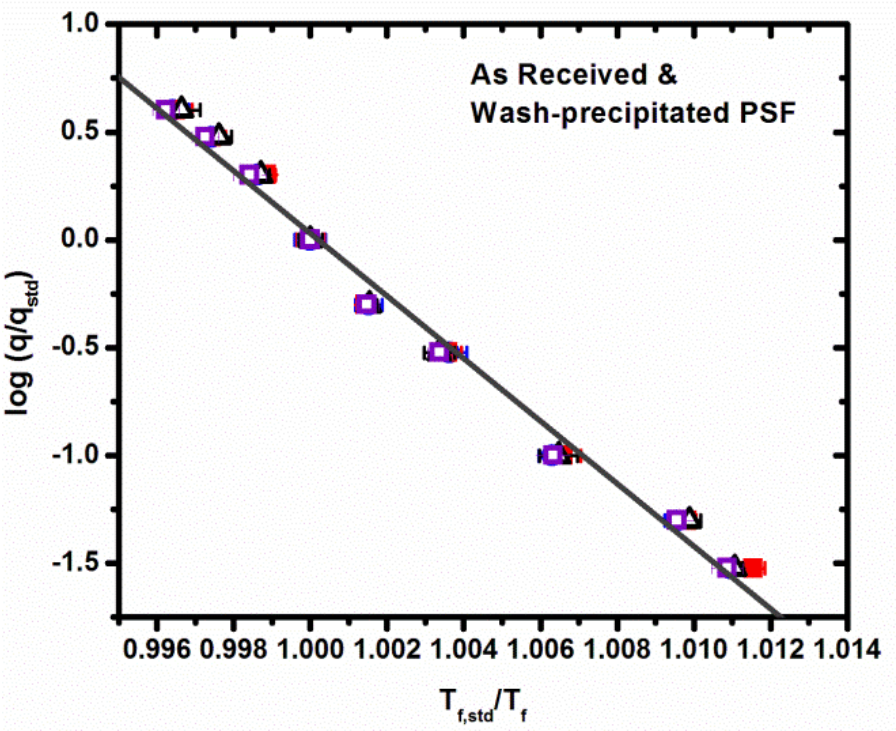

Figure 4.4 Arrhenius plot of the reduced cooling rate vs. the reciprocal of the reduced fictive temperature for the as-received and the wash-precipitated PSF at heating rate of 10 ^{o}C/min.

DSC scans on the as-received and the wash-precipitated PSF were also performed at a constant heating rate of 20 ^{o}C/min using the same broad range of cooling rates (40 to 0.3 ^{o}C/min) that were used to perform the DSC scans at constant heating rates of 10 ^{o}C/min. The dynamic fragility was found to be $m = 145 \pm 3$, which is consistent with the results for the experiments at 10 ^{o}C/min heating rate.

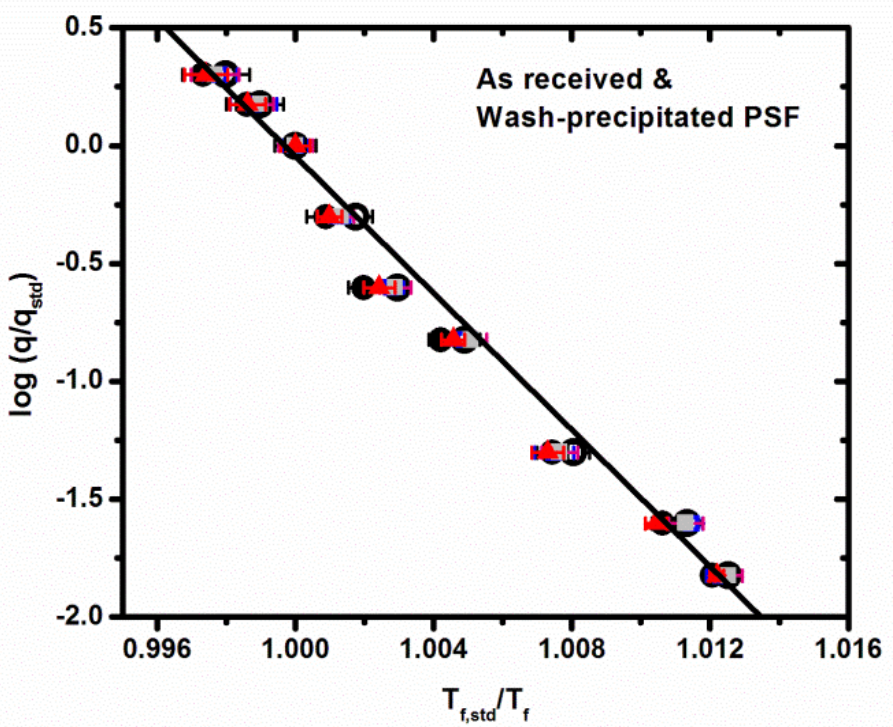

Figure 4.5 The reduced cooling rate vs. the reciprocal of the reduced fictive temperature for the as-received and the wash-precipitated PSF at heating rate of 20 ^{o}C/min.

The current dynamic fragility of $m = 145 \pm 3$ is in good agreement with the previously reported value of $m = 149$ from Labahn *et al.*[70] by dielectric measurements. However, $m = 145 \pm 3$ is in disagreement with the value reported by Evans *et al.*[55] of $m = 286 \pm 25$ for their wash-precipitated PSF. If only the limited range of cooling rates from our study is considered, the dynamic fragility (Figure 4.6) is $m = 180 \pm 6$ which is higher than $m = 145 \pm 3$, but still much smaller than the $m = 286 \pm 25$ reported by Evans *et al.*[55]

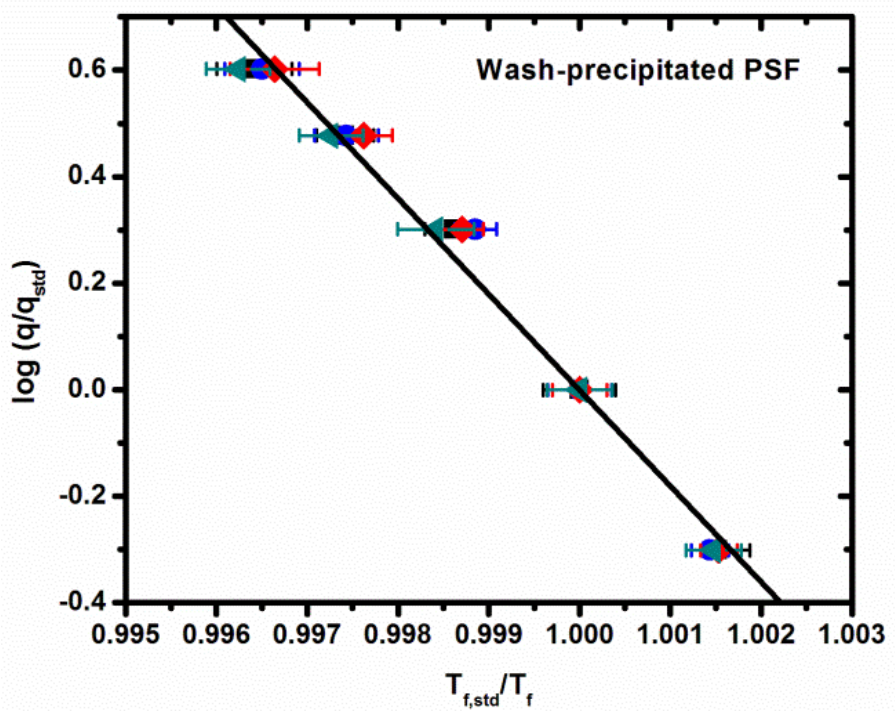

Figure 4.6 Arrhenius plot of the short range of cooling rates (5 to 40 °C/min) vs. the reciprocal of the fictive temperature for the wash-precipitated PSF samples at a heating rate of 10 °C/min.

4.4.1.2.2 Bisphenol-A-Polycarbonate (PC)

DSC scans on the as-received and the wash-precipitated PC were also performed at a constant heating rate of 10 ^{o}C/min using the same broad range of cooling rates (40 to 0.3 ^{o}C/min) that were used to study the other polymers. The obtained dynamic fragility is 130 ± 2 (Figure 4.7) for the broad range of high cooling rates and 170 ± 4 for the limited range of cooling rates. In both the scenarios where the heating rates were at 10 ^{o}C/min and 20 ^{o}C/min for the as-received or the wash-precipitated PC, the dynamic fragility was much smaller than that reported by Evans *et al.*[55] (m = 277 ± 25 for their wash-precipitated PC or m = 204 ± 25 for their as-received PC). The current study results are consistent with literature fragility values reported for PC via creep experiments (m = 119 or 132)[72,73] and DRS (m = 175)[74,75] and DSC (m = 102 ± 8) [63]. The reported m = 102 ± 8 [63] corresponds to a study with a much broader range of cooling rates (nine cooling rates) by using a conventional DSC and a flash DSC measurements.[63,77]

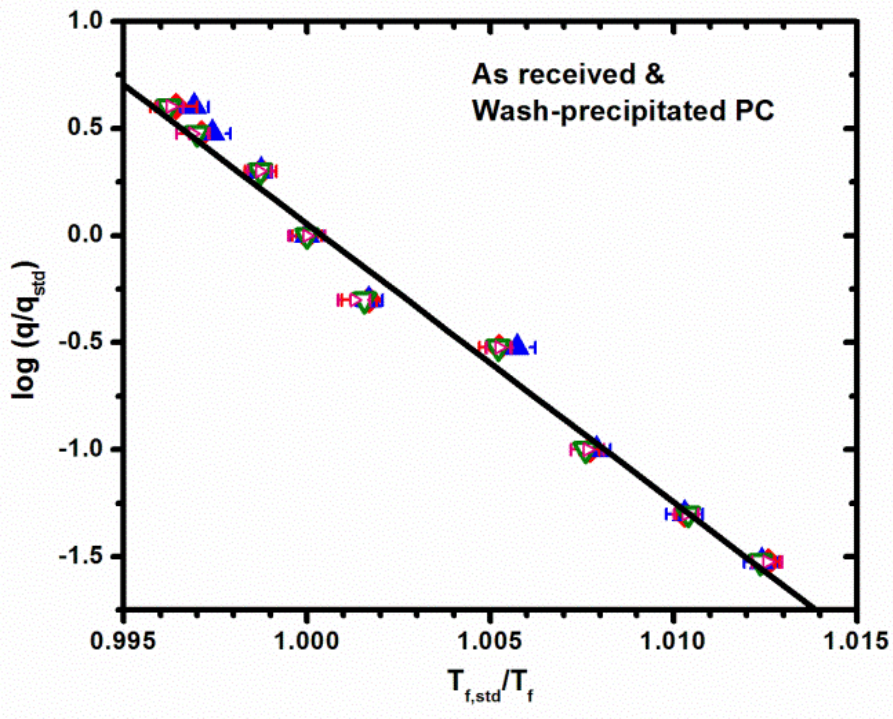

Figure 4.7 The reduced cooling rate vs. the reciprocal of the reduced fictive temperature for the as-received and the wash-precipitated PC at heating rate of 10 ^{o}C/min and 20 ^{o}C/min.

4.4.1.2.3 Polyvinyl Chloride (PVC)

For the as-received and the wash-precipitated PVC, the obtained dynamic fragility (Figure 4.8) was 180 ± 3 for the broad range of cooling rates at heating rates of 10 or 20 ^{o}C/min. Current results are consistent with the literature result of m = 191 via creep compliance, but do not agree with the value of m = 317 reported by Evans *et al.*[55]

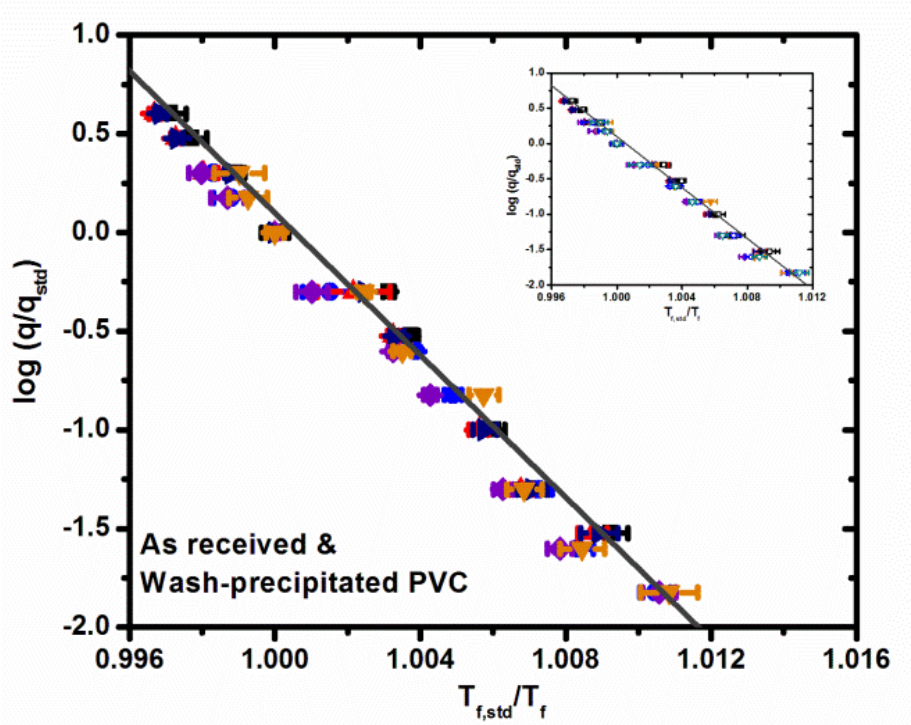

Figure 4.8 Plot of the reduced cooling rate vs. the reciprocal of the reduced fictive temperature for the as-received and the wash-precipitated PC at heating rate of 10 ^{o}C/min and 20 ^{o}C/min.

4.4.1.3 Possible Reasons for Differences between Current Study and Evans et al.[55] Work

As mentioned, Evans *et al.*[55] used a smaller range of high cooling rates (5, 10, 20, 40 ^{o}C/min) for their determination of the dynamic fragility. However, we were not able to obtain their extremely high values. One possible reason for the extremely high fragility values found by Evans *et al.*[55] in their work on PSF, PC, and PVC might be attributed to an improper calculation on the determination of the fictive temperature. Evans *et al.*[55] claimed to have used Moynihan's area matching method for the determination of the T_f. However, their described procedure was based on drawing the glassy line from a given point in the glassy state parallel to the liquid state line (Figure

4.9). While the correct interpretation for the Moynihan's method is to draw a line for the C_{pg} equation deep in the glassy state (red line in Figure 4.9) and a line for the C_{pl} equation (blue line in Figure 4.9). Therefore, Evans *et al.*[55] seem to have miscalculated T_f by means of incorrect interpretation of Moynihan's method, therefore introducing error in the obtained value of the dynamic fragility. By using Evans et al.[55] data (Figure 4.9), the fictive temperature would be 102.7 ºC and by using the correct slope for the C_{pg} and C_{pl} the fictive temperature is 103.9 ºC. The difference between Evans *et al.*[55] fictive temperature and the fictive temperature found in the current study does not seem to diverge much from one another as to explain the disagreement on the dynamic fragility values obtained by Evans *et al.*[55] and current results.

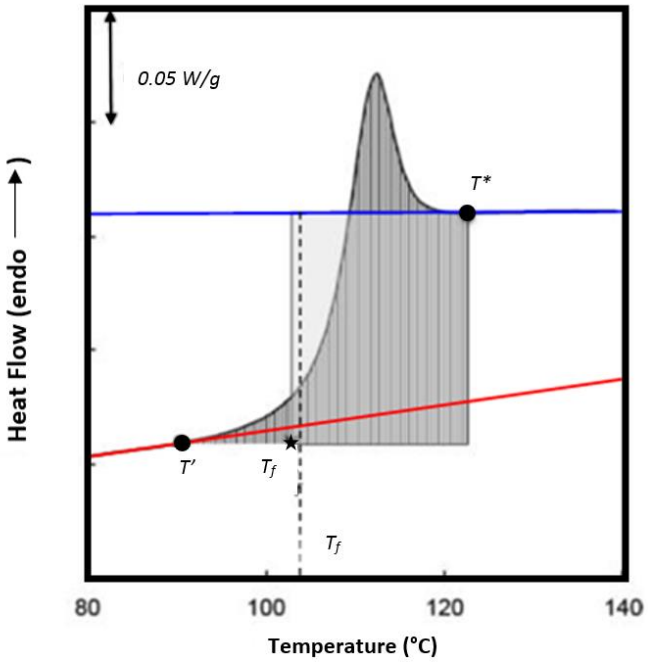

Figure 4.9 Illustration taken from Evans *et al.*[55] for one of their polystyrene sample at a cooling rate of 5 ºC/min and heating rate of 20 ºC/min. The red and blue lines were added to the original illustration.

4.4.2 Rheology Measurements

4.4.2.1 Lactic Acids

The steady shear viscosity for the D,L-lactic acid (Figure 4.10) is shown for experimental temperatures ranging from T_g + 3 to T_g + 50 ^oC.

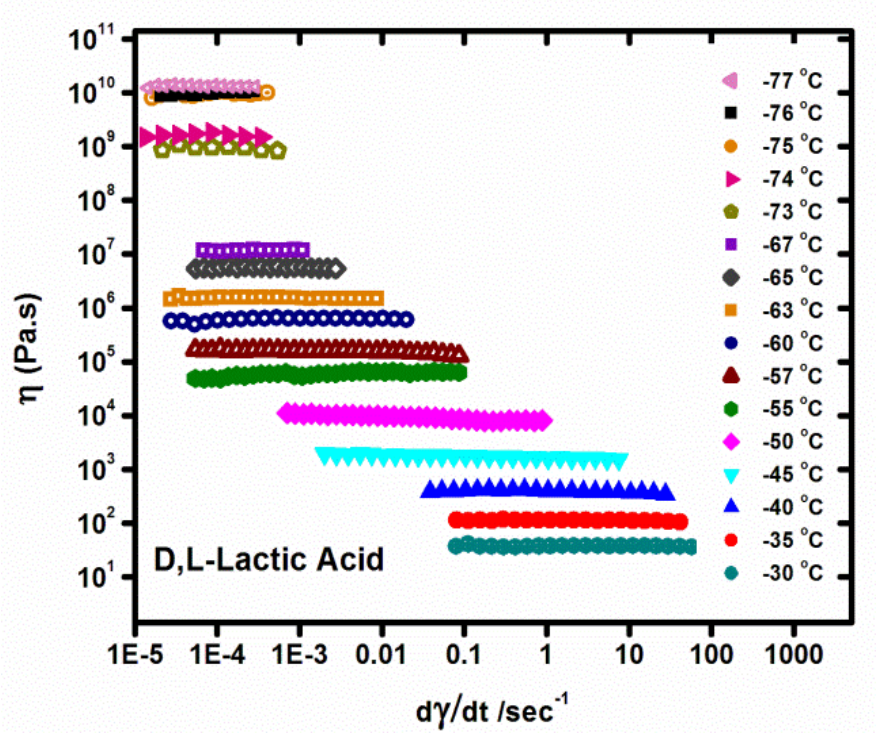

Figure 4.10 Zero shear viscosity for D,L-lactic acid at experimental temperatures ranging from T_g + 3 to T_g + 50 ^oC.

The average viscosity at each temperature (Figure 4.11) was used to fit the VFT equation, and the dynamic fragility was obtained. The dynamic fragility was found to be *m* = 78. The dynamic fragility for D,L-lactic acid is much smaller than the dynamic fragility of the decalin (*m* = 145) material reported by Wang *et al*.[52] They speculated that the dynamic fragility of the lactic acid should be much larger than the dynamic fragility of decalin. However, via calorimetric or rheological methods the *m* of lactic acid is found, here, to be smaller than that of decalin.

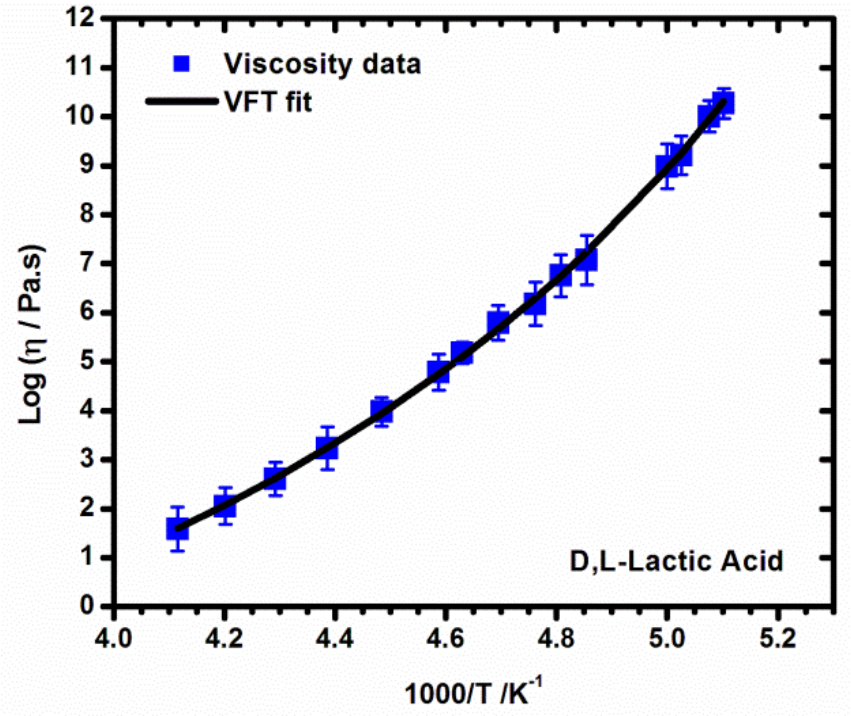

Figure 4.11 D,L – lactic acid viscosity vs. the reciprocal of temperature. Solid line represents the VFT fit.

4.4.2.2 Bulk Polymer

4.4.2.2.1 Polysulfone (PSF)

Only the as-received and the wash-precipitated PSF materials were used to investigate the fragility using dynamic frequency sweep measurements. The storage (Figure 4.12 and Figure 4.13) and the loss (Figure 4.14) moduli were obtained and the master curves created by using the temperature superposition. The reference temperature was chosen to be 186 ^{o}C. The shift factors used to construct the master curves were used to obtain the dynamic fragility by fitting the data to both the VFT and the WLF equations. Figure 4.13 shows an insert of both master curves of the storage modulus for the as-received and the wash-precipitated PSF, which can be seem to closely overlap. Similarly, Figure 4.14 shows the master curves of the loss modulus

for the as-received and the wash-precipitated PSF, and these two curves also closely overlap.

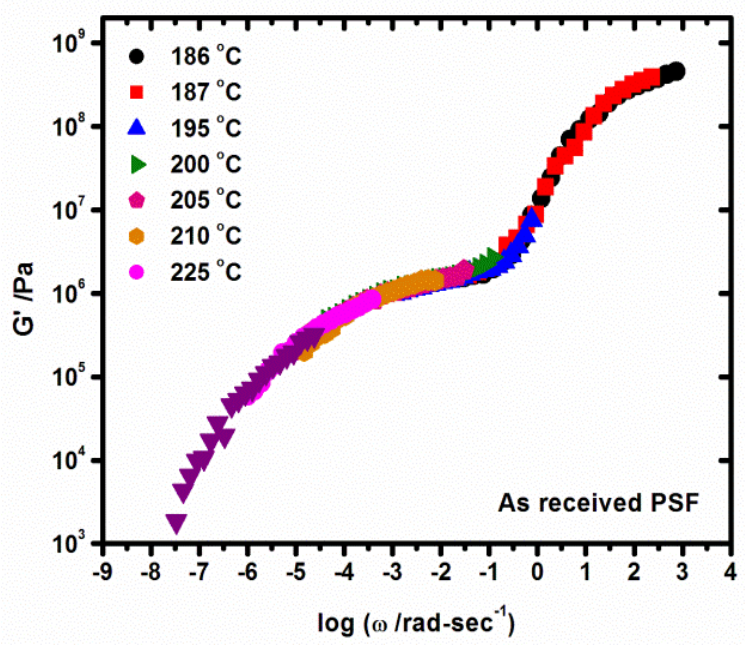

Figure 4.12 Storage modulus as a function of frequency for the as-received PSF. The master curve was obtained from the frequency-temperature superposition with T_{ref} of 186 °C.

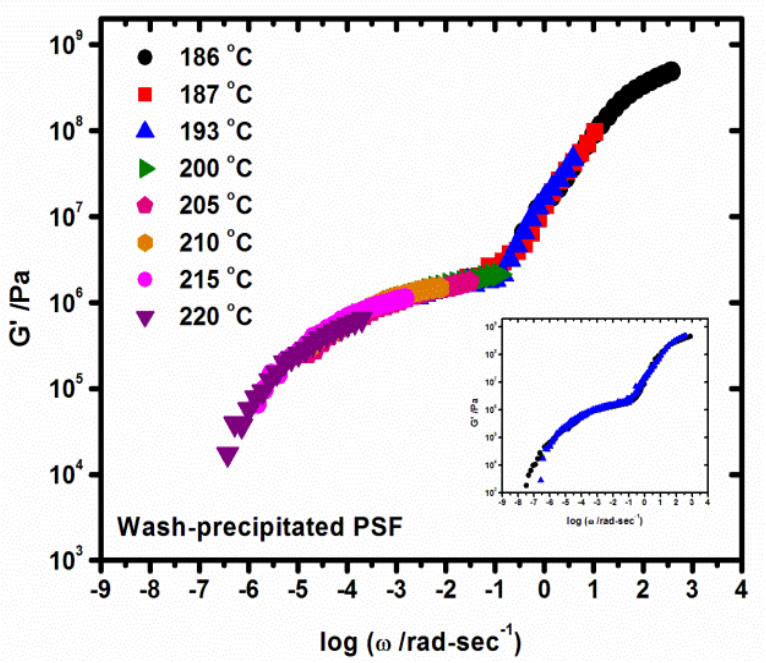

Figure 4.13 Master curve of storage modulus as a function of frequency for the wash-precipitated PSF with T_{ref} of 186 °C. The insert compares the master curves of the as-received (squares) and the wash-precipitated (triangles) PSF.

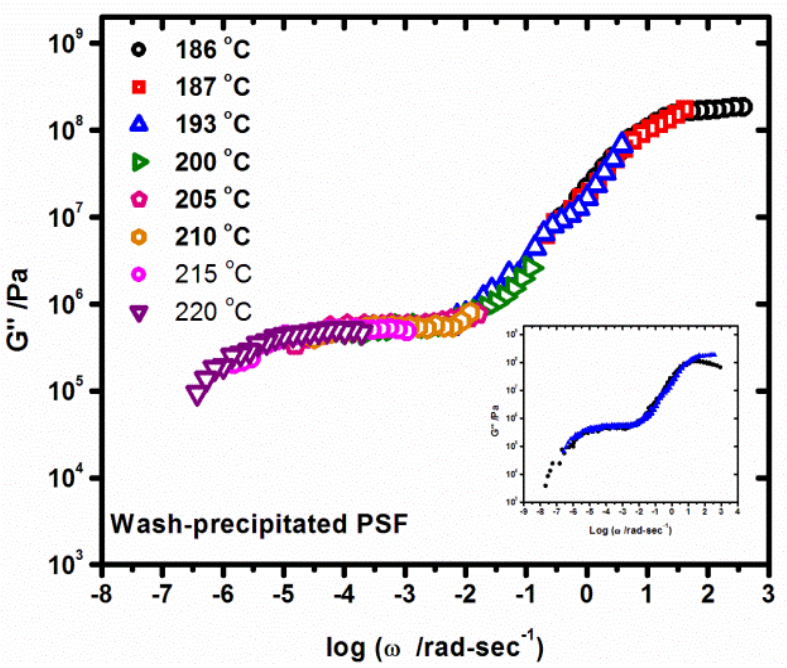

Figure 4.14 Master curve of loss modulus for the wash- precipitated PSF with T_{ref} of 186 °C. Insert compares wash-precipitated (triangles) with as-received (circles) PSF master curves.

From the horizontal shift factors used to construct the master curve of the storage and the loss moduli (Figure 4.12, 4.13, and 4.14), the VFT[6-8] equation was used to obtain the dynamic fragility of m = 144 ± 9 and 150 ± 7 for the as-received and the wash-precipitated PSF, respectively. The dynamic fragilities obtained from the rheological studies and the dynamic fragility found from the calorimetric studies (m = 145 ± 3) are consistent with each other. The dynamic fragility can also be found by using the WLF expression. The obtained fragilities from the WLF[9] fit were obtained to be (m = 140 ± 8) for the as-received PSF with C_1 and C_2 of 12 and 39 ºC and (m = 148 ± 5) for the wash-precipitated PSF with C_1 and C_2 of 12 and 37 ºC. These obtained C_1 and C_2 values from the current study are similar to literature values for PSF with C_1 and C_2 of 15.6 and 53.4 ºC with an experimental temperature ranging from T_g to T_g + 100 ºC and using T_g = 186 ºC.[4]

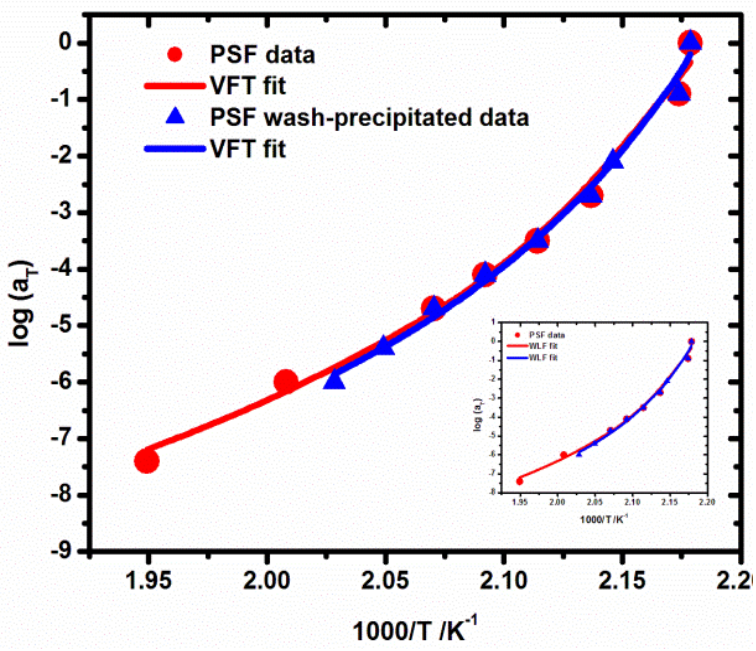

Figure 4.15 Shift factors used to construct the master curves of the as-received and the wash-precipitated PSF. The solid lines represent the VFT fit to the data. The insert shows the shift factors being fitted by the WLF equation.

4.5 Discussion

4.5.1 Polymer Fragilities

There were two main motivations in the current study, one of them was to examine if there are polymers (PC, PSF, PVC) with dynamic fragilities higher than *m* = 214. The second motivation was to examine the possibility that the dynamic fragility of a polymer can in fact change if the polymer is used as-received or after wash-precipitation. The reason is that work from Evans et al.[55] not only reported the extreme high dynamic fragility values for PSF, PC, and PVC, but they also related the high values to the sensitivity of the T_g to the film thickness in supported films.

Our findings indicate that the as-received and the wash-precipitated polymer have the same dynamic fragility values, meaning *m* is independent of the treatment. Furthermore, our dynamic fragility values are within the range of literature results for similar polymers, but not in agreement with the ones reported by Evans *et al.*[55] There are other two important aspects worth of discussion. The first is an observation reported by Santangelo and Roland[79] about how the molecular weight of the polymer affects the fragility of polymers. While this is true, the molecular weight dependence gets weak once the T_g becomes fairly independent of molecular weight[48,79-82]. Furthermore, the differences in molecular weight between the polymers used by us and the ones used by Evans *et al.*[55] are not substantial. Hence, this cannot be the cause for the extreme differences between the Evans *et al.*[55] results and those found by us in the present study.

The second aspect worth of discussion is the one discussed by Evans *et al.*[55], that the increase in dynamic fragility is associated with wash-precipitating the polymer. For example, Evans *et al.* [55] reported that PSF has *m*=124 if used as-received and *m*=286 if used after wash-precipitation, however, the T_g itself did not vary more than about 1 ºC. However, in a work by Zheng *et al.*[57] on pure poly(α-methyl styrene) and a mixed of poly(α-methyl styrene) with its hexamer, the temperature dependence and activation energies of the segmental shift factors were determined. The dynamic fragility obtained from the determined data suggested that the pure polymer had a fragility of 190 while the 50/50 mixture of the polymer and the oligomer is approximately 90. Furthermore, the changes in the fragility were based in large changes in the glass transition temperature observed between the pure polymer and the 50/50 mixture. However, these large changes in the glass transition temperature due to the plasticization were not reported in either the Evans *et al.*[55] work or seen in the present work.

Of interest is a dynamic fragility value reported by Robertson *et al.*[48] on PVC (*m* = 267). This dynamic fragility was obtained from calorimetric data originally presented by Hodge.[83,84] However, same calorimetric studies were performed by Pappin *et al.*[18] in the same PVC (M_n of 65 kg/mol and PDI of 3.15) batch used by Hodge[83,84]. However, the dynamic fragility obtained by Pappin *et al.*[85] was 164 when using a broad range of cooling rates (160 to 0.5 K/min). In the current investigation, it was observed that the short range of high cooling rates used by Evans *et al.*[55] (5, 10, 20, 40 ºC/min) tends to give a higher *m* than when using a broader range of cooling rates

(0.3, 0.5, 1, 3, 5, 10, 20, 30, 40 ºC/min). Pappin *et al*.[85] did not comment on the differences in slopes at high and low cooling rate ranges. However, these different slopes at low and high cooling rates are also observed in the Pappin *et al*.[85] work on PVC. These slopes on Pappin *et al*.[85] data were obtained by using the Arrhenius law as in the current work. The dynamic fragility for PVC is 146 when using cooling rate data from 0.5 to 40 K/min. However, when the cooling rates ranging from 5 to 160 K/min are used, *m* is 197. By using the same range of cooling rates as the one used by Evans *et al*.[55] for PVC, *m* is 170. In none of these scenarios, an extreme dynamic fragility value was obtained.

As mentioned previously in the current paper, the fictive temperature was measured incorrectly by Evans *et al*.[55]. For example, a small error in fictive temperature can result in a considerable large error in the obtained *m* when only the limited and high cooling rate range is used. Hence it seems plausible that a significant portion of the high fragilities obtained by Evans, *et al*.[55] might be due to errors in fictive temperature induced by either the improper procedure of measuring fictive temperature.

4.6 Conclusions

Calorimetric studies were used to determine the dynamic fragility of lactic acids: D,L-lactic acid and D-lactic acid. The dynamic fragility by means of calorimetric methods was obtained from the T_g (fictive temperature used instead) dependence on cooling rate as suggested by Wang *et al.*[52] The value of the fragility was then obtained from the slope of the line by plotting the reduced cooling rate vs. the reciprocal of the reduced fictive temperature. The dynamic fragilities of the lactic acids were $m = 80 \pm 2$ and $m = 86 \pm 2$ for the D,L-lactic acid and the D-lactic acid, respectively. From the temperature dependence of the zero shear rate viscosity, the dynamic fragility of D,L-lactic acid was $m = 78$. The dynamic fragility obtained by calorimectry or rheology shows consistent results, but these results for the lactic acids do not support the speculated results by Wang *et al.*[52] that D,L-lactic acid should exhibit an extremely high fragility.

In the case of the as-received or the wash-precipitated PSF, PC, and PVC polymers, the results show that the dynamic fragility values obtained in the present investigation are consistent with previously reported literature results. However, they do not agree with the reported results by Evans *et al.*[55] who reported extremely high fragility values for wash-precipitated polymers. In the current work, the as-received PSF or the wash-precipitated PSF dynamic results either by calorimetric or rheological measurements show consistent results. Dynamic fragilities were 145 ± 3 (as-received and wash-precipitated PSF) by calorimetric methods and between 144 ± 9 (as-received PSF) and 150 ± 7 (wash-precipitated PSF) by rheological methods. Our current results

show consistent *m* values with that previously reported by Labahn with *m* = 149 by DRS.[63] The *m* values from the current study do not agree with the extremely high dynamic fragility value of 286 ± 25 reported by Evans *et al.*[55] using calorimetry. For the PC and PVC polymers in the present work, *m* was found to be 130 ± 2 and 180 ± 3, respectively via calorimetric studies. These current dynamic values for PC and PVC do not reproduce *m* values of 277 ± 25 (wash-precipitated PC), 204 ± 25 (as-received PC), or 317 ± 35 (wash-precipitated PVC) reported by Evans *et al.*[55] Some of the possible reasons for the extremely high fragilities reported by Evans *et al.*[55] might be related to the small range of cooling rates (5, 10, 20, and 40 ^{o}C/min) used to determine the dynamic fragility. In the case of PC, Evans *et al.*[55] presented large fragility values for both their as-received PC and wash-precipitated PC. However, in the current study our range of cooling rates was broader using nine cooling rates from 0.3 to 40 ^{o}C/min resulting in m = 130 ± 2. Similarly Shamim *et al.*[63] also reported a dynamic fragility m = 102 ± 8 (smaller than the one in current work) and they worked with a much broader range of cooling rates ranging from 0.3 K/min to 1000 K/s by using conventional and flash DSC. The other possible reason might be the improper interpretation and implementation of the Moynihan's area matching method to determine the fictive temperature at different cooling rates at a constant heating rate. However, these do not fully account for the extreme values reported by Evans *et al.*[55]

CHAPTER 5

CONCLUSIONS AND FUTURE WORK

5.1 Conclusions

In the first part of the study, the T_g dependence on polymeric film thickness was obtained by means of the liquid dewetting method. The liquid dewetting method can be used to dewet a single polymer film at a fixed temperature or to dewet a single polymer film sample under consecutive temperature-steps. The advantage of the latter procedure is to minimize the number of samples used and to still be able to obtain the same dewetting information. Results from the liquid dewetting method showed that the T_g dependences on thicknesses are different from those for rigid substrate supported films or freely standing films reported in the literature. However, the T_g dependence on h seems to follow more closely the behavior of the supported films than the freely standing films. Furthermore, the dewetting behaviors of a 3 arm star polystyrene and a linear polystyrene were similar in nature and showed the same T_g reduction with decreasing h. However in the case of the 8 arm star PS ($M_{n,branch}$ = 10 kg/mol) the behavior is quite different.

In current work, the dynamic fragility values of D,L-lactic acid, D-lactic acid, PSF, PC, and PVC were investigated. For D,L-lactic acid and PSF, the dynamic fragilities were obtained by means of calorimetric and rheological methods. For all other materials *m* was obtained only by calorimetric methods. One of the main motivations of the current work was to determine if the dynamic fragility for a

polymer varies if the polymer receives a wash-precipitation treatment. Evans *et al.*[55] reported that the dynamic fragility values of the wash-precipitated PSF, PC, and PVC vary from that of the as-received polymers. The current study shows that the dynamic fragility did not vary as reported by Evans *et al.*[55] On the contrary, the dynamic fragility values stay unchanged if the material is used as-received or after a wash-precipitation treatment. It was also observed that the dynamic fragility obtained by using a limited range of cooling rates vs. a broad range of cooling rates makes the *m* vary. Higher *m* values were observed when using the limited range of high cooling rates, but these higher values were not as higher as those reported by Evans *et al.*[55] One main problem with the Evans et al.[55] work was their interpretation of how to calculate the fictive temperature while trying to use the Moynihan area matching method. While this incorrect interpretation introduced errors to the calculated fictive temperatures, it is improbable that these differences could of have caused such an increase in the dynamic fragility. The second motivation was to investigate whether D,L-lactic acid has an extreme high dynamic fragility as expected by Wang *et al.*[52] In this particular case, *m* for the lactic acid was obtained by means of calorimetric and rheological measurements, and it was observed that in both studies the obtained dynamic fragilities of the lactic acid were relatively consistent with each other and not close to the dynamic fragility of decalin.

5.2 Future work

Future work related to current studies on liquid dewetting of polystyrene films might include:

- Liquid dewetting experiments to obtain the T_g – film thickness behavior on star branched polystyrenes with different functionalities and molecular weights (e.g. f = 4, f = 8 with M_n per arm higher than 57 kg/mol). As it was observed, that the 3 arm star PS had same T_g – film thickness response as the linear PS films. However, the two 8 arm star polystyrenes with 10 kg/mol per arm and 57 kg/mol per arm showed a more complex behavior. Both 8 arm star PS samples showed consistent T_g – film thickness behavior with each other, but in both cases the T_g response was different than the linear and the 3 arm star PS films. For that particular reason it is of interest to understand the dynamics of the functionality of the star arm polystyrene on the T_g.

- Liquid dewetting studies on a broad range of molecular weights for different polystyrene architectures like pom-pom polystyrene, comb polystyrene, hyperbranched polystyrene. This is recommended since current studies show that architecture and molecular weight might play a role on the T_g response.

- Liquid dewetting measurements using other liquid substrates (e. g. the ionic liquid used by Wang *et al.*[52]) on the polystyrene with different architectures and other polymers that might be suitable for a negative spreading parameter.

Future work related to current studies on dynamic fragility might include:

- Rheological methods on PC, PVC, and D-lactic acid to obtain the dynamic fragility and to directly compare those results to the dynamic fragility obtained from thermal methods.
- Deeper investigation on the actual effect of wash-precipitation treatment on the dynamic fragility of polymers.
- Further investigation on the effect of short range of high cooling rates compared to a more broad range of cooling rates either by conventional DSC or by flash DSC.

BIBLIOGRAPHY

1 McKenna, G. Glass Formation and Glassy Behavior. *Pergamon Press plc, Comprehensive Polymer Science: the Synthesis, Characterization, Reactions & Applications of Polymers.***1989**, *2*, 311-362.

2 Jackson, C. L.; McKenna, G. The Glass Transition of Organic Liquids Confined to Small Pores, *J. Non-Cryst. Solids* **1991**, *221*, 131-133.

3 Badrinarayanan, P.; Zheng, W.; Li, Q.; Simon, S. L. The Glass Transition Temperature versus the Fictive Temperature. *J. Non-Cryst. Solids* **2007**, *353*, 2603-2612.

4 Ngai, K. L.; Plazek, D. J. in Physical Properties Handbook, edited by J. E. Mark (American Institute of Physics, Woodbury, NY) **1996**, pg. 139-160,341.

5 Alcoutlabi, M.; McKenna, G. M. Effects of Confinement on Material Behavior at the Nanometer Size Scale. *J. Phys- Condens. Matter*, **2005**, *17***,** R461-524.

6 Vogel, H. Temperature Dependence Law of the Viscosity of Liquids. *Z. Phys.*, **1921**, *22*, 645-646.

7 Tamman, G.; Hesse, W. Z. The Dependence of the Viscosity on the Temperature of Undercooled Liquids. *Z. Anorg. Allg. Chem.*, **1926**, *156*, 1, 245-257.

8 Fulcher, G. S. Analysis of Recent Measurements of the Viscosity of Glasses. *J. Am. Ceram. Soc*., **1925**, *8 (6)*, 339-355.

9 Williams, M. L.; Landel, R. F.; Ferry, J. D. The Temperature Dependence of Relaxation Mechanisms in Amorphous Polymers and Other Glass-Forming Liquids. *J. Am. Chem. Soc.***1955**, *77 (14)*, 3701-3707.

10 Tool, A. Q. Relation between Inelastic Deformability and Thermal Expansion Glass in its Annealing Range. *J. Am. Chem. Soc.***1946**, *29*, 240-253.

11 Richardson, M. J.; Savill, N. J. Derivation of Accurate Glass Transition Temperatures by Differential Scanning Calorimetry. *Polymer* **1975**, *16*, 753-757.

12 Moynihan, C. T.; Easteal, A. J.; Wilder, J.; Tucker, J. Dependence of the Glass Transition Temperature on Heating and Cooling Rate. *J. Phys. Chem.* **1974**, *78(26)*, 2673-2677.

13 Moynihan, C. T.; Easteal, A. J.; DeBolt, M. A.; Tucker, J. Dependence of the Fictive Temperature of Glass on Cooling Rate. *J. Am. Ceram. Soc.* **1976**, *59*, 12-16.

14 Keddie, J. L., Jones, R. A. L.; Cory, R. A. Interface and Surface Effects on the Glass-Transition Temperature in Thin Polymer Films. *Faraday Discuss.* **1994**, *98*, 219-230.

15 Keddie, J. L.; Jones, R. A. L. Glass-Transition Behavior in Ultra-Thin Polystyrene Films. *Is. J. Chem.* **1995**, *35*, 21-26.

16 Keddie, J. L., Jones, R. A. L.; Cory, R. A. Size-Dependent Depression of the Glass Transition Temperature in Polymer Films. *EPL (Europhys. Lett.)* **1994**, *27*, 59.

17 Forrest, J. A., Dalnoki-Veress, K.; Dutcher, J. R. Interface and Chain Confinement Effects on the Glass Transition Temperature of Thin Polymer Films. *Phys. Rev. E.* **1997**, *56*, 5705.

18 Forrest, J. A.; Dalnoki-Veress, K. The Glass Transition in Thin Polymer Films. *Adv. Colloid Interface Sci.* **2001**, *94*, 167-195.

19 Kawana, S.; Jones, R. A. L. Character of the Glass Transition in thin Supported Polymer Films. *Phys. Rev. E.* **2001**, *63*, 02150 (1-6).

20 Fakhraai, Z.; Forrest, J. A. Probing Slow Dynamics in Supported Thin Polymer Films, *Phys. Rev. Lett.* **2005**, *95*, 02570(1-4)

21 Bäumchen, O.; McGraw, J. D.; Forrest, J. A.; Dalnoki-Veress, K. Reduced Glass Transition Temperatures in Thin Polymer Films: Surface Effect or Artifact? *Phys. Rev. Lett.* **2012**, *109*, 055701.

22 Glynos, E.; Frieberg, B.; Green, P. F. Wetting of a Multiarm Star-Shaped Molecule. *Phys. Rev. Lett.* **2011**, *107*, 128303(1-5).

23 Glynos, E.; Frieberg, B.; Oh, H.; Liu, M.; Gidley, D. W.; Green, P. F. Role of Molecular Architecture on the Vitrification of Polymer Thin Films. *Phys. Rev. Lett.* **2011**, *106*, 128301.

24 Mattsson, J.; Forrest, J. A.; Börjesson, L. Quantifying Glass Transition Behavior in Ultrathin Free-Standing Polymer Films. *Phys. Rev. E.* **2000**, *62*, 5187.

25 Dalnoki-Veress, K.; Forrest, J. A.; Murray, C.; Gigault, C.; Dutcher, J. R. Molecular Weight Dependence of Reductions in the Glass Transition Temperature of Thin Freely Standing Polymer Films. *Phys. Rev. E.* **2001**, *63,* 031801.

26 O'Connell, P. A.; McKenna, G. B. Rheological Measurements of the Thermoviscoelastic Response of Ultrathin Polymer Films. *Science* **2005***, 307,* 1760-1763.

27 O'Connell, P. A.; McKenna, G. B. Dramatic Stiffening of Ultrathin Polymer Films in the Rubbery Regime. *Eur. Phys. J. E* **2006**, *20(2),* 143-150.

28 O'Connell, P. A.; McKenna, G. B. Novel Nanobubble Inflation Method for Determining the Viscoelastic Properties of Ultrathin Polymer Films. *Rev. Sci. Instrum.* **2007**, *78,* 013901(1-11).

29 O'Connell, P. A.; McKenna, G. B. A Novel Nano-bubble Inflation Method for Determining the Viscoelastic Properties of Ultrathin Polymer Films. *Scanning Vol.* **2008**, *30,* 184-196.

30 O'Connell, P. A.; Hutcheson, S. A.; McKenna, G. B. Creep Behavior of Ultra-Thin Polymer Films. *J. Polym. Sci., Part B: Polym. Phys.* **2008**, *46,* 1956-1965.

31 Pye, J. E.; Roth, C. B. Two Simultaneous Mechanisms Causing Glass Transition Temperature Reductions in High Molecular Weight Freestanding Polymer Films as Measured by Transmission Ellipsometry. *Phys. Rev. Lett.* **2011**, *107,* 235701.

32 Bodiguel, H.; Fretigny, C. Viscoelastic Properties of Ultrathin Polystyrene Films. *Macromolecules* **2007**, *40,* 7291-7298.

33 Bodiguel, H.; Fretigny, C. Reduced Viscosity in Thin Polymer Films. *Phys. Rev. Lett.* **2006**, *97,* 266105 (1-4).

34 Bodiguel, H.; Fretigny, C. Viscoelastic Dewetting of a Polymer Film on a Liquid Substrate. *Eur. Phys. J. E* **2006**, *19,* 185-193.

35 Wang, J.; McKenna, G. B. Viscoelastic and Glass Transition Properties of Ultrathin Polystyrene Films by Dewetting from Liquid Glycerol. *Macromolecules* **2013**, *46,* 2485-2495.

36 Wang, J.; McKenna, G. B. A Novel Temperature- Step Method to Determine the Glass Transition Temperature of Ultrathin Polymer Films by Liquid Dewetting. *J. Polym. Sci., Part B: Polym. Phys.* **2013**, *51,* 1343-1349.

37 Lu, H.; Chen, W.; Russell, T. P. Relaxation of Thin Films of Polystyrene Floating on Ionic Liquid Surface. *Macromolecules* **2009**, *42*, 9111-9117.

38 Forrest, J. A.; Dalnoki-Veress, K.; Stevens, J. R.; Dutcher, J. R. Effect of Free Surfaces on the Glass Transition Temperature of Thin Polymer Films. *Phys. Rev. Lett.* **1996**, *77*, 2002.

39 Xu, S.; O'Connell, P. A.; McKenna, G. B. Unusual Elastic Behavior of Ultrathin Polymer Films: Confinement-Induced/Molecular Stiffening and Surface Tension Effects. *J. Chem. Phys.* **2010**, *132*, 184902.

40 McKenna, G. B. Confinement III. Summary and Perspectives on Dynamics in Confinement. *Euro. Phys. J. – Spec. Top.* **2007**, *141*, 291-301.

41 Wang, J. The Viscoelastic Property of Thin Films. Ph.D. Dissertation, Texas Tech University, Lubbock, TX, 2013

42 Fryer, D. S.; Peters, R. D.; Kim, E. J.; Tomaszewski, J. E.; De Pablo, J. J.; Nealey, P. F Dependence of the Glass Transition Temperature of Polymer Films on Interfacial Energy and Thickness. *Macromolecules.* **2010**, *43*, 9937-9944.

43 Mapesa, E. U.; Erber, M.; Tress, M.; Eichhorn, K. J.; Sergheri, A.; Voit, B.; Kremer, F. Glassy Dynamics in Nanometer Thin Layers of Polystyrene. *The Euro. Phys. J – Spec. Top.* **2010**, *189*, 173-180.

44 Raegen, A.; Massa, M.; Forrest, J.; Dalnoki-Veress, K. Effect of Atmosphere on Reductions in the Glass Transition of Thin Polystyrene Films. *Euro. Phys. J. E: Soft Matter* **2008**, *27*, 375-377.

45 Angell, C. A. Relaxation in Liquids, Polymers and Plastic Crystals – Strong/Fragile Patterns and Problems. *J. Non-Cryst. Solids* **1991**, *(131-133)*, 13-31.

46 Hodge, I. M. Strong and Fragile Liquids – A Brief Critique. *J. Non-Cryst. Solids* **1996**, *202*, 164-172.

47 Richert, R.; Angell, C. A. Dynamics of the Glass-Forming Liquids. V. On the Link Between Molecular Dynamics and Configurational Entropy. *J. Chem. Phys.* **1998**, *108*, 9016-9026.

48 Robertson, C.G.; Santangelo, P.G.; Roland, C. M. Comparison of Glass Formation Kinetics and Segmental Relaxation in Polymers. *J. Non-Cryst. Solids* **2000**, *275*, 153-159.

49 Huang, D.; McKenna, G. B. New Insights into the Fragility Dilemma in Liquids *J. Chem. Phys.* **2001**, *114(13)*, 5621-5630.

50 Martinez, L.-M.; Angell, C. A. A Thermodynamic Connection to the Fragility of Glass-Forming Liquids. *Nature* **2001**, *410*, 663-666.

51 Crowley, K. J.; Zografi, G. The use of Thermal Methods for Predicting Glass-Former Fragility. *Thermochim. Acta* **2001**, *380*, 79-93.

52 Wang, L. M.; Velikov, V.; Angell, C. A. Direct Determination of Kinetic Fragility Indices of Glassforming Liquids by Differential Scanning Calorimetry: Kinetics versus Thermodynamic Fragilities. *J. Chem. Phys.* **2002**, *117 (22)*, 10184- 10192.

53 Huang, D.; Colucci, D. M.; McKenna, G. B. Dynamic Fragility in Polymers: A Comparison in Isobaric and Isochoric Conditions. *J. Chem. Phys.* **2002**, *116(9)*, 3925-3933.

54 Qin, Q.; McKenna, G. B. Correlation between Dynamic Fragility and Glass Transition Temperature for Different Classes of Glass Forming Liquids. . *Non-Cryst. Solids* **2006**, *352*, 2977-2985

55 Evans, C. M.; Deng, H.; Jager, W. F.; Torkelson, J. M. Fragility is a Key Parameter in Determining the Magnitude of T_g – Confinement Effects in Polymer Films. *Macromolecules* **2013**, *46*, 6091-6103.

56 Shamim, N.; McKenna, G. B. Glass Dynamics and Anomalous Aging in a Family of Ionic Liquids above the Glass Transition Temperature. *J. Phys. Chem.* **2010**, *114*, 15742-15752.

57 Zheng, W.; McKenna, G. B.; Simon, S. L. The Viscoelastic Behavior of Polymer/Oligomer Blends. *Polymer* **2010**, *51(21)*, 4899-4906.

58 Collins, T. J., ImageJ for microscopy. *Biotechniques* **2007**, *43 (1)*, 25-30.

59 Owens, D. K., Some Thermodynamic Aspects of Polymer Adhesion. *J. Appl. Polym. Sci.*, **1970**, *14 (7)*, 1725-1730.

60 Graf, K.; Kappl, M., *Phys. Chem. of interfaces*. John Wiley & Sons: **2006**.

61 Owens, D. K.; Wendt, R. C. Estimation of the Surface Free Energy of Polymers. *J. Appl. Polym. Sci.* **1969**, *13*, 1741-1747.

62 Kwok, D. Y.; Neumann, A. W. Contact Angle Interpretation: Re-evaluation of Existing Contact Angle Data. *Colloids Surf., A: Physicochem. Eng. Asp.* **2000**, *161*, 49-62.

63 Shamim, N.; Koh, Y. P.; Simon, S. L.; McKenna, G. B. Glass Transition Temperature of Thin Polycarbonate Films Measured by Flash Differential Scanning Calorimetry. *J. Polym. Sci., Part B: Polym. Phys.* **2014**, *52(22)*, 1462-1468.

64 Struik, L. C. E. Physical Aging in Amorphous Polymers and other Materials, Elsevier North-Holland Inc., **1978**; Chapters 2-4.

65 Hutcheson, S. A.; McKenna, G. B. The Measurement of Mechanical Properties of Glycerol, m-Toluidine and Sucrose Benzoate Under Consideration of Corrected Rheometer Compliance: An in-Depth Study and Review *J. Chem. Phys.* **2008**, *129*, 074502(1-14)

66 Simon, S. L. Enthalpy Recovery of Poly(ether imide): Experiment and Model Calculations Incorporating Thermal Gradients. *Macromolecules* **1991**, *30,* 4056-4063.

67 Simon, S. L. Enthalpy Recovery of Poly(ether imide): Experiment and Model Calculations Incorporating Thermal Gradients. *Macromolecules* **1991**, *30,* 4056-4063.

68 Simon, S. L.; Plazek, D. J., Sobieski, J. W.; McGregor, E. T. Physical Aging of a Polyetherimide: Volume Recovery and Its Comparison to Creep and Enthalpy Measurements. *J. Polym. Sci., Part B: Polym. Phys.* **1997**, *35(6)*, 929-936.

69 Echeverria, I.; Su, P.-C.; Simon, S. L.; Plazek, D. J. Physical Aging of a Polyetherimide: Creep and DSC Measurements. *J. Polym. Sci., Part B: Polym. Phys.* **1995**, *33*, 2457-2468.

70 Labahn, D.; Mix, R.; Schönhals, A. Dielectric Relaxation of Ultrathin Films of Supported Polysulfone *Phys. Rev. E* **2009**, *79*, 011801(9).

71 He, Y. Y.; Lutz, T. R.; Ediger, M. D.; Ayyagari, C.; Bedrov, D.; Smith, G. D. NMR Experiments and Molecular Dynamics Simulations of the Segmental Dynamics of Polystyrene. *Macromolecules* **2004**, *37,* 5032-5039.

72 Mercier, J. P.; Aklonis, J. J.; Litt, M.; Tobolsky, A. V. Viscoelastic Behavior of Polycarbonate of Bisphenol A *J. Appl. Polym. Sci.* **1965**, *9,* 447-459.

73 Böhmer, R.; Ngai, K. L.; Angell, C. A.; Plazek, D. J. Nonexponential Relaxations in Strong and Fragile Glass Formers. *J. Chem. Phys.* **1993**, *99,* 4201.

74 Heydemann, P.; Guicking, H. D. *Kolloid-Z. Z. Polym.* **1963**, *193 (16)*, 16-25.

75 Kaufmann, S.; Wefing, S.; Schaefer, D.; Spiess, H. W. J. Two-dimensional Exchange Nuclear Magnetic Resonance of Powder Samples. III. Transition to Motional Averaging and Application to the Glass Transition. *J. Chem. Phys.* **1990**, *93*, 197-214.

76 Kauzmann, W. The Nature of the Glassy State and the Behavior of Liquids at Low Temperatures. *Chem. Rev.* **1948**, *43 (2)*, 219-256

77 Koh, Y. P.; Simon, S. L. Structural Relaxation of Stacked Ultrathin Polystyrene Films *J. Polym. Sci., Part B: Polym. Phys.* **2008**, *46*, 2741-2753.

78 Debenedetti, P. G.; Stillinger, F. H. Supercooled liquids and the glass transition. *Nature* **2001**, *410*, 259-267.

79 Santangelo, P. G.; Roland, C. M. Molecular Weight Dependence of Fragility in Polystyrene *Macromolecules*, **1998**, *31*, 4581-4585.

80 Ding, Y.; Novikov, V. N.; Sokolov, A. P.; Cailliaux, A.; Dalle-Ferrier, C.; Alba-Simionesco, C.; Frick, B. Influence of Molecular Weight on Fast Dynamics and Fragility of Polymers. *Macromolecules*, **2004**, *37*, 9264-9272.

81 Andreozzi, L.; Faetti, M.; Giordano, M.; Zulli, F. Molecular-Weight Dependence of Enthalpy Relaxation of PMMA. *Macromolecules*, **2005**, *38*, 6056-6067.

82 Hintermeyer, J.; Herrmann, A.; Kahlau, R.; Goiceanu, C.; Rössler, E. A. Molecular Weight Dependence of Glassy Dynamics in Linear Polymers. *Macromolecules*, **2008**, *41*, 9335-9344.

83 Hodge, I.M. Effects of Annealing and Prior History on Enthalpy Relaxation in Glassy Polymers. 1. Experimental Study on Poly (Vinyl Chloride). *Macromolecules*, **1982**, *15*, 756-761

84 Hodge, I.M. Effects of Annealing and Prior History on Enthalpy Relaxation in Glassy Polymers. 4. Comparison of five polymers. *Macromolecules*, **1983**, *16*, 898-902.

85 Pappin, A. J.; Hutchinson, J. M.; Ingram, M. D. Enthalpy Relaxation in Polymer Glasses: Evaluation and Interpretation of the Tool-Narayanaswamy Parameter X for Poly(Vinyl chloride). *Macromolecules*, **1992**, *25*, 1084-1089